UNIVERSITY POLITEHNICA OF BUCHAREST
Faculty of Material Science and Engineering
Department of Metallic Materials Science, Physical Metallurgy

No. Senate .....Decision in . .2020

DOCTORAL THESIS SUMMARY

Silver doped and undoped Hydroxyapatite Coatings of Medical Alloy for Biomedical Applications

Author: *Drd. eng.* Mohammed Alqasim Fayeq Khazaal Alsabti

By *Supervisor*

Prof. dr. ing. Ion CIUCĂ

DOCTORAL COMMITTEE

President	Prof. Univ. Habil. Dr. Ing. Antoniac Vasile Iulian	Politehnica University of Bucharest
Coordinator	Prof. Univ. Dr. Ing. Ciucă Ion	Politehnica University of Bucharest
Referent	Prof. Univ. Dr. Ing. Popa Cătălin	Tehnica University of Cluj-Napoca
Referent	Prof. Univ. Dr. Ing. Șerban Viorel-Aurel	Politehnica University of Timișoara
Referent	Prof. Univ. Dr. Ing. Ghiban Brândușa	Politehnica University of Bucharest
Referent supleant	Prof. Univ. Dr. Ing. Nicoară Mircea	Politehnica University of Timișoara
Referent supleant	Prof. Univ. Habil. Dr. Ing. Miculescu Florin	Politehnica Universoty of Bucharest

Bucharest 2020

Table of Contents

Acknowledgments

In the name of Allah, the most Beneficent and the most Merciful.

All praises be to ALLAH for providing me with the persistence, the patience and all the blessings which made this work possible in spite of the current situation in my home country of Iraq.

This thesis is the result of research conducted over a period of about four years during my PhD studies at ***University of Politehnica, Bucharest- Romania (UBP)***. I have been studied at the Faculty of Material Science and Engineering., and I am deeply grateful that I was given the opportunity to perform research in the field of Metallurgy Engineering. During my PhD journey I have had valuable opportunities to attend conferences and write scientific publications and thesis. It is my opinion that good work has been accomplished in the PhD studies, and I have been aiming to conduct experimental work to obtain more validating results. My research work is on-going, and I will 'InShaAllah' continue my research in this area which is nanocoatings of biomaterials.

I would like here to express my gratitude , great pleasurea , my sincere, thanks and gratefulness to my supervisor ***Prof. dr. ing. Ion CIUCĂ*** for his supports, advice, motivation, enthusiasm, and immense knowledge which made this experience fruitful and enjoyable, I am greatly appreciated. Moreover, I would like to present my thanks to the head of advanced structural characterization Laboratory seniour Researcher Ph.D ***Bogdan Stefan Vasile***, ***Roxana Trusca*** and all faculty/ staff members of the Departments/ Center.

My heartfelt thanks and sense of gratitude are to my family members; father, mother, sisters and brother for their prayer, patience and continuing dedicated support.

Mohammed Alqasim
2020

INTRODUCATION

The urgent need which imposed by imposed by the new world realities on human that leads him to reflection and research in all the scientific and material possibilities available which has it, in order to reach the common target of developing materials and methods for service of humanity especially people's health.

The thesis aimed to "biomaterial development" by biomaterials surface modification depending on coating by hydroxyapatite doped and undoped silver on the surfaces of famous implant medical alloys like **Ti6Al4V** alloy and **Co-Cr-Mo** alloy, after a required surface treatment consists of creating the roughness using a blasting process which depends on different sizes of alumina particles (19, 45, 110, 250 μm) .

sol-gel technique was used as a liquid phase to precipitate the multiple layers of thin nanofilms with hydroxyapatite doped and undoped silver on rough surfaces of medical alloys to obtain thin films adhered to surface, then the morphology of surface was studied before and after of hydroxyapatite doped and undoped silver coating by using the Scanning Electron Microscope SEM in order to evaluate the shape and distribution of particles, as well as the study of atomic and crystalline structures showed by X-ray diffraction XRD.

Bioactivity and biocompatibility can be seen as important properties for medical alloys, In any case, in order to indicate their response in environments which they operate in them. Technique of simulating body fluid SBF have been used by immersion the samples of alloys in solution similar to human blood plasma in terms of ionic concentration for 7, 14 and 21 days, after that, the differences of phases formed, their distribution and structures can be observed by X-ray diffraction and scan electronic microscope for both of hydroxyapatite doped and undoped silver coating with different roughness obtained as mentioned above.

On the other hand, the interface of tissue and biomaterial is an appropriate environment for bacterial colonization. Therefore, the technique of incorporating silver nanoparticles into hydroxyapatite was used to increase the coating effectivity against bacteria by precipitation of silver ion coatings of ion exchange, then the biofilm activity evaluated by using P.seudomonas aeruginosa, then study the effect of it on biomaterial before and after coating and the role of roughness through changing of surface topography on the growth of microorganisms ,as well as, evaluation of cellular compatibility or cell survival by using MTT method for its effect on biofilm production.

The results showed the important of roughness to enhance the hydroxyapatite doped and undoped silver coating on medical alloy surfaces of **Ti6Al4V** alloy and **Co-Cr-Mo** alloy, by another side to support the implant as an important antimicrobial agent, as well as enhancing the adhesion and bonding between surface of cobalt-chromium-molybdenum alloy and hydroxyapatite doped and undoped silver coating, which it was a barrier due to the dissolution and the breakdown of the hydroxyapatite layer. In same time, the crystalline structures having a positive effect in increasing the effectivity of the hydroxyapatite doped and undoped silver coating.

High roughness of **Ti6Al4V** alloy coated by hydroxyapatite which contain of bioactive apatite structure characterized of bone repair or implantation transplants that is what apatite owned of high stability in terms of biocompatibility and bioactivity as result of uniform and homogeneous distribution of deposited layers, in addition to their positive influence in bacterial resistance and biofilms formation at Pseudomonas aeruginosa.

The importance of silver incorporated with hydroxyapatite, where silver released as ions which enhance the role of biofilms against the microbial attack, it is understood that the interfaces between the hydroxyapatite and the biomaterial more susceptible to microbial attack.in addition to, the activity of antibacterial increased with increased the roughness of surface where the surface area increases and becomes less solubility, which will be as better contact with microorganisms.

The calcium phosphate compounds formed at high roughness of cobalt- chromium-molybdenum alloy surfaces, which plays significant part in the stability of composition, bonding with biomaterial, compatibility and high bioactivity.

The results of the comparison between the **Ti6Al4V** and the **Co-Cr-Mo** of high roughness

showed the formation of "HAp $Ca_5(PO_4)_3(OH)$ and $Ca_3(PO_4)_2$ TCP" sequentially, despite their role in biocompatibility, but the HAp characterized to be less Solubility and less bone absorption, while TCP has more soluble and non-bone used to bone repair which disappears by resorption gradually.

MOTIVATION OF THE RESEARCH

Implantable medical alloys such as **Ti6Al4V** alloy and **Co-Cr-Mo** have a multi properties which allowed it to work in the environment of human body for protracted periods. Especially in terms of the biocompatibility, bioactivity, corrosion resistant and possess excellent mechanical properties when they relate to use in load-bearing implants. As well as for resistant to microbial.

Even though, technical modifications of surface improvements have been studied by academic researchers to some medical alloys, However, The urgent need a further studies be undertaken in these areas, in order to achieve safety medical alloys. That depends on selection of materials and processing less expensive.

Modifying the surfaces by forming bioactive nanocoating on implantable medical alloys is necessary to improve the bioactivity and biocompatibility, which is making these alloys more safety in medical applications for long-term implantation.

RESEARCH STRATEGY

Research strategy is strategies that are utilized for the quest for look into or the path chose to take care of the examination issue efficiently. Research is the craft of logical and methodical examination for pertinent data on a particular part of information. Along these lines, when we use the term look into technique, we don't just mean the strategies utilized, yet in addition the rationale behind the techniques utilized.

Through the current study of thesis, behavior of experimental was taken place to study the research issues which treated in the thesis. Research vision depends on the processes and procedures applied systematically, as indicated below:

1. Literature review: A writing overview was performed to characterize the scientific research, and the gaps of information for field of implant alloys, protective coating by conventional methods and protective nanocoating by thin films.
2. Required surface treatment as a technique to obtained the different surface roughness by using grit-blasting process to increase the bond between coating and surface.
3. Advanced nanocoating methods: rarely, technique of spin coating used to employ hydroxyapatite on to biomaterials implants for deposition thin films with high quality and uniformity in sub-nanometer scale of thickness.
4. Characterize of the thin films by (SEM, XRD) before and after coating as well as biological characterization by antimicrobial tests and cellular viability.
5. Stabilization of thin films of hydroxyapatite can be based on practical bio-mimicry by immersing implants in the "simulated body fluid", in addition to, observation the morphology of samples surface which coated using scanning electron microscope and analysis the microstructures with X-ray spectra after immersion.
6. Antibacterial metal ion resistance: Ag ion is used as antimicrobials incorporated with HA coatings which is the effective route to get antibacterial properties by coating to form regular division of Ag particles in the coatings through the microorganisms growth of materials attendance and biofilm production.

SCOPE AND LIMITATIONS

The thesis included the following major issues related to research work:

1. Studying a high quality of hydroxyapatite as a thin film formed by coating a different medical **Ti6Al4V** and **Co-Cr-Mo** alloy surfaces using sol-gel mrthod by spin coating.
2. Characterizing the nanocoating thin films by, XRD, SEM.

3. Studying the alloy surface roughness effects on the microstructure and crystal structures of surface.
4. Studying the biocompatibility by immersion in SBF then characterize by XRD and SEM and bioactivity of thin films formed by planktonic microorganisms growth of immersion samples and biofilm production.

THESIS ORGANIZATION

The current thesis has been divided into five chapters and it can be specified as follows:

Chapter 1. Introduction: this chapter includes the research overview of biomaterials and offers a literature study showing the development of surface modifications methods used for implant alloys. Besides, it contains the research motivation, research strategy and purpose of research, as well as explaining the organization of thesis.

Chapter 2. Theoretical Background: Gives theoretical background included Ti6Al4V and Co-Cr medical alloys types and properties, Nanotechnology , Nanocoatings, and sol-gel derived HA , Spin coating method as advanced method to formed thin films.

Chapter 3. Experimental Work: Covers the experimental tests carried out using methods and techniques of formed layer, characterizations and applications.

Chapter 4.Results and Discussion: addressed the results achieved with discussions on details.

Chapter 5. Conclusions and Further Research: Summarized the results that have been reached with recommendation of further research.

The bibliography is representative and modern; containing reference papers in the studied domain, and is composed of **221** titles.

CHAPTER 1: INTRODUCATION OF BIOMATERIALS

1.1. INTRODUCTION

Biomaterials which are directly interacting with living tissues or biological systems, whether they are natural or a synthetic materials, which are subject to the physical, biological study, and level of interaction with the human body, grouped under the name of biomaterial science [1]. Historically, With reference to the date of 1895, more than 100 years, for used the first bone of metal plate "steel plate" to fix the fracture of bone, the researcher Lane is credited it [2][3]. Mechanical behavior, biocompatibility and corrosion resistance in fluids and tissues of body are the biomaterials key requirements [4][5]. Biocompatibility is the materials ability of contact with bodily fluids and tissues, without creating unintended ,damaging results and unacceptable of body's harm. such as toxicity and irritating effect, inflammatory and allergic reaction, and mutagenic or carcinogenic [6][7]. For that the metals implants should be biologically active and chemical inert [7] Biomaterials included "the metals, ceramics, polymers, and composite".

1.2. BIOMATERIALS

Definition of biomaterials depends on the materials which can used for replacement of body organs and body functions [8].

1. Technical Definition **2.** Surgical term definition

1.3. CLASSIFICATION OF BIOMATERIALS

1. Natural Biomaterials: like Proteins, Gelatin, Silk, Fibrin, Cellulose, Chitin, Chitosan [9],[10],[11].
2. Synthetic biomaterials : which are produced in a lab or in an industry with human effects are called as synthetic biomaterials contain :

- ✓ Metal and alloys biomaterials (Biometal).
- ✓ Polymer biomaterials.
- ✓ Ceramic biomaterials

1.4. CLASSIFICATION IMPLANT OF MATERIALS

1. Bioinert Materials
1. Bioactive Materials
2. Bioresorbable Materials

1.5. BIOMATERIALS CHARACTERISTICS

1. Biofunctionality
2. Biocompatibility

1.6. REVIEW OF LITERATURE

It deals with the previous works divided into two groups: Titanium alloy coated by HAP and HAp_Ag and the other for Co-Cr-Mo coated with HAP and HAp_Ag.

CHAPTER 2: THEORETICAL STUDY OF BIOMEDICAL ALLOYS

2.1. MEDICAL ALLOYS

Medical alloys which represent the materials that are manufactured for use in various medical fields; repair or bone implants and medical devices, because of the mechanical, physical and medical properties they possess such as biocompatibility, bioactivity and corrosion resistance. As well as these alloys enable to interact with the biological medium and tissues for a long time, among the most famous of these alloys :

- Titanium alloys **Ti-6Al-4V**
- Cobalt based alloys **Co-Cr-Mo**
- Stainless steel alloy **316L**

There is still a need to develop these alloys in order to reduce manufacturing costs, good features suitable for the human body, working for a long time and solve some of the problems facing manufacturing processes[12] [13] [14] [15].

2.2. TITANIUM ALLOYS

Titanium alloys are now the most attractive metallic materials for biomedical applications. In medicine, they are used for implant devices replacing failed hard tissue. Examples include artificial hip joints, artificial knee joints, and bone plates, screws for fracture fixation, cardiac valve prostheses, pacemakers, and artificial hearts. **Ti-6Al-4V** has long been a main medical titanium alloy. However, for permanent implant applications the alloy has a possible toxic effect resulting from released vanadium and aluminum. For this reason, vanadium- and aluminum-free alloys have been introduced for implant applications, based on the **Ti-6Al-4V** implants" [16][17].

2.2.1. Titanium alloy of biomaterials

These new alloys include Ti-6Al-7Nb (ASTM F1295), Ti-13Nb-13Zr (ASTM F1713), ,Ti-12Mo-6Zr (ASTM F1813) and Ti6Al4V which used most widely as hard tissue replacement in artificial bones, joints and dental implants [18][19]**.**

2.2.2. Chemical composition and phase transformation

This alloy considered that contains of α+β along with 6 wt. % of aluminum that achieves the stabilizing a-phase, while 4 wt. % of vanadium achieves the stabilizing β-phase.

2.2.3. Mechanical properties

The mechanical properties of Ti6Al4V medical alloys can be affected by the microstructure of their constituent.

2.2.4. Corrosion resistance

Ti-6Al-4V alloy have excellent corrosion resistance and good biocompatibility for these used for many years as implants materials [20]. significant problems occurred such as long-term performance which due to failed of prostheses and necrosis in tissues [21]**.**

2.2.5. Biomedical applications

Ti6Al4V alloy is commonly used for fabrication of several forms of implants or devices that are surgically implanted in human body. They are used of medical application and biocompatibility by implanting of replacing devices failed of the hard tissue

2.3. COBALT BASED ALLOYS

The development of the cobalt-chromium alloys is credited to "Elwood Haynes", where patent was issued on 1907, In the name of "Satellite alloys". In addition to using a suitable alloying elements such as tungsten and molybdenum to enhancement the mechanical properties of **Co-Cr-Mo** alloys as result of the properties of **Co-Cr-Mo** based alloy such as superior strength, high hardness, high wear feature, good corrosion resistance and biocompatibility enabled it to engage into the biomedical world as materials in orthopaedic and dental implants, also **Co-Cr-Mo** alloy successfully demonstrated as load-bearing of joint replacement surgery which reported through the last forty years as in "hip" and "knee" replacement devices

2.3.1. ASTM of Co-Cr-Mo Alloys

The CO-Cr alloys of surgical implants are classified as ASTM-13, which is medical and surgical materials and devices set by the American Society of Testing and Materials (ASTM) based on chemical, mechanical and metallurgical requirements. ASTM F75, ASTM F1537 and F799 are the most important types of Co-Cr-Mo alloys.

2.3.2. Co-Cr-Mo phase diagrams

Pure cobalt is stable with crystalline face structure FCC known as (γ-Co) above 417°C but loses its stability and transformation from metastable state at 417°C to the thermodynamically stable of HCP hexagonal closed packed structure as (ε-Co) below 417°C, At 1495 °C, the pure cobalt transformation to liquidus phase, and with normal rates of cooling, the liquidus phase turns to martensite slowly [22] [23].

2.3.3. Microstructure

The overall picture determine the grains forming the material and the arrangement of the crystals according to the crystal lattices in space, as well as the grain boundaries that represent the sites of high energy with large atomic distortions as obstacles to further propagation of dislocations. In addition to the grains shape and grains distribution.

The microstructure of the material according to the aforementioned is a great importance to determining the identity of the material, since the microstructure of the material affected by mechanical treatments and heat treatments and thus affects the overall mechanical, physical and chemical properties of the material.

2.3.4. Mechanical properties

On the basis of manufacturing process for **Co-Cr-Mo** alloy and its chemical constituents, multiphase structures, age hardening by precipitation of carbides, the mechanical properties are excellent and good wear resistance, good biocompatibility and high harness comparable with Ti alloys. The mechanical properties for Co-Cr alloys which depend on the manufacturing process

2.3.5. Biomedical Applications

Two forms of Co-Cr alloys as casting alloys and wrought classifications used for biomaterial applications of five alloys according to ASTM [24] as shows in ***Table 2.1.*** the applications and properties [25] [26] [27] [28]**.**

Table 2.1. show the applications and properties of Titanium alloys ypes.

ASTM system	Types of alloy	Applications	Properties
ASTM F75 Co-28Cr-6Mo	casting alloy	Stem, ball, cup of artificial joints, Fixation screws and Bone plates	High resistance to corrosion, good mechanical, strength, fatigue and wear resistance, and biocompatibility. Good castability and hot workability.
ASTM F799, : F1537 Co-28Cr-6Mo	thermodynamically processed alloy	Joint replacements (hip, knee, shoulder and Fixation devices	High corrosion resistance, high temperature resistance, non-magnetic
ASTM F90 Co-20Cr-15W-10Ni	wrought alloy	manufacture the biomedical implants, balloon-expandable stents, Fixation wires, Vascular stents and Heart valves	Machinability, excellent strength, biocompatibility, hot, cold workability and good ductility.
ASTM F562 Co-35Ni-20Cr-10Mo	wrought alloy	Lead conductor wires, Springs, Stylets, Orthopedic cables Catheters, Orthopedic cables and cardiovascular stents	High fatigue strength and high modulus of elasticity.
ASTM F1058 40Co-20Cr-16Fe-15Ni-7Mo	wrought alloy	Arch wires, Springs, Lead conductor wires, Surgical clips, Balloon-expandable stents (annealed) and Self-expanding stents (aged)	good workability and wear resistance and good fatigue strength

2.4. COATING AND MODIFICATION BIOMATERIALS

Bone cells adhered to the surface coated with apatite without formed any overlapping when implants of metal coated by hydroxyapatite, the surface of the hydroxyapatite of the bone cells becomes an integral part of the hydroxyapatite coating. This represents the good adhesion of the bone to coated implant [29][30]. biomaterials surface coatings are a way of encapsulating metal to be accepted in the human body when implanted[29]. For the purpose of coating the biomaterial , the coating process is necessary to be proportionate with the substrate, so the substrate should be maintained properly during the process as is the case with titanium and its alloys

There are several techniques used in coating surfaces of bio-metallic materials, including:

- Hydroxyapatites coating.
- Tricalcium phosphate glass-ceramic coatings.
- beta-tricalcium phosphate
- Oxide coatings
- Composite coatings.

After surgical procedure, implant surface exposed to post-operative infections by the bacteria attached to the implant surface, which later form biofilm at the implant site, which it is necessary to prevent the biofilm formed before they become very resistant to immune response and antibiotics [31]. Silver and its ions are characterized by antimicrobial activity by cation of silver inhibiting resistance of bacteria with offer low toxicity of human cells Through this characteristic of silver has drawn attention to the development of the coating of HAp containing silver [44],[45][34][35], for the purpose of antimicrobial effectiveness, the low concentration of Ag^{+} released from Ag doped

hydroxyapatite which used while the high concentration cause cytotoxicity [36][37].

2.4.1. Calcium phosphates

Agroup of minerals containing calcium ions (Ca^{2+}) together with orthophosphates (PO_4^{3-}), metaphosphates ($P_2O_7^{4-}$) and occasionally hydrogen or hydroxide ions [38]. Based on their composition, CaP play a significant role in human bodies and other mammals as they represent the inorganic part of healthy bones and teeth as well as pathological calcified tissues [39].

2.4.2. Hydroxyapatite

Hydroxyapatite is a bioactive compound [40] it is represented by its chemical composition $Ca_{10}(PO_4)_6(OH_2)_2$ similar to the bone mineral [2],[3]. it is known that the bone is a composition of natural organic minerals consisting of two basic compounds collagen and hydroxyapatite [43] as a result of this, they are used in orthopedic, dental, and maxillofacial applications [44].so used as a preferred coating for metal implants to improve surface properties [45].

The preferred coating of hydroxyapatite is the result of the chemical, structural and biological similarity of the human body, its ability to interact with the tissue surrounding it [46] .the biological apatite of bone is represented by Ca^{2+} and OH^- without carbonated hydroxyapatite with different ions within the crystalline network or within the non-apatite such as Mg^{2+}, Na^+, K^+, Zn^{2+}, F^-, Cl^- and HPO_4^{2-} [47] where the Biological, physicochemical and mechanical properties of apatite increases with the of the incorporation of ions [48] , hydroxyapatite is used directly with bone repair and for unloaded implants and dental implants , while it is used as a coating when the surface of metal exposed to the loads such as titanium alloys and cobalt / chromium alloys and magnesium alloys [49][50][51][52].

The benefits of hydroxyapatite when utilizing for coated **Ti6Al4V** alloy represented by:

1. rapidly incorporated into the human body where hydroxyapatite connect to bone forming indiscernible unions [53] which hasten bone growth around the implant [54] this is known (bioactive coating) [55]..
2. High osteoconductivity due to promote bone regeneration [56] which depends on thermodynamically stable at physiological pH and actively property for strong chemical bonds with the surrounding bone [57]**.**
3. Due to the weakness of the mechanical properties of most porous calcium phosphate materials, the excellent mechanical properties found in the metallic substrates are exploited [58].
4. Has a chemical composition comparable to human bone natural [59].
5. Hydroxyapatite coating was also reported to decrease the metal ion release[60].

2.4.3. Methods for hydroxyapatite synthesis

There are two ways to obtain hydroxyapatite, the first is through natural sources such as eggshells, seashells , animal bones such as bovine cortical bone and plants, which are the most common sources of similarity with the mineral component of bone biological due to the morphological and structural similarity of the human bone [13],[14], the other from inorganic synthesis [63] which consist some processing methods include:

1. Dry methods
2. Wet methods
3. High temperature processes

Sol-gel technique used to prepare a colloidal system which containing the medium of a liquid dispersion in "spatial grid" created by combined particles of "dispersed phase". knowing that materials of sol-gel process include the "nanomaterials" , also the colloidal system built on the idea of sol transformation into a gel [64].

The variety of synthesis methods of materials made from solutions, that fall under the common name of "sol-gel process", As is known, the gel considered as the one of the outcomes of process steps. the most important steps of sol-gel process related to hydrolysis of compounds like " M(OR)x (M = Si, Ti, Zr, V, Zn, Al, Sn, Ge, Mo, W, etc.)' and the chlorides in an aqueous or

organic environment as" alcohol" [65].

2.4.4. Spin Coating:

A method to prepare films from a dissolved/dispersed substance by removing the solvent with high speed spinning [66], the spin coating is used to depositing uniform thin layers on the surface of the material [67], the solution to be used is used in an excess quantity on the surface of the material either manually by a syringe or automatically with the distribution unit and the discharge nozzles in the lid of the spin coater [68]. The material is then rotated at a high speed (e.g. up to 10.000 rpm) In order to ensure distribution of fluid by centrifugal force. The device used for spin coating is called spin coater and spin processor or simply spinner [69]**.**

The process of spin coating undergo for four various stages which include deposition, spin up, spin off and evaporation Specifications:

1. Used for preparation of ultrathin films with high degree of smoothness[70]
2. Widely used[67]
3. Totally reproducible[71]
4. Also capable of preparing submonolayer “open” films[72]
5. Thick films also possible, although with a larger roughness[73]

CHAPTER 3. EXPERMENTAL WORK

3.1. PRACTICAL PROCEDURES

This practical procedures included, selection of material which contain both of **Ti6Al4V** and **Co-Cr-Mo** alloy, then preparation of the specimens to obtained the roughness surfaces, synthesis of hydroxyapatite doped and undoped Silver, coating method of thin film on surfaces of **Ti6Al4V** and **Co-Cr-Mo** alloy, as well as, evaluation and characterization methods by SEM and XRD analysis, Stabilization of thin films in SBF, and Biological characterization.

3.1.1 Hydroxyapatite solution undoped and doped silver

Hydroxyapatite solution undoped and doped silver content were prepared, respectively in nine days according to the following stages of technical flow as shown in ***figure 3.1***. using a necessary laboratory instruments, equipments and materials which used to prepare the two solution of hydroxyapatite doped and undoped silver

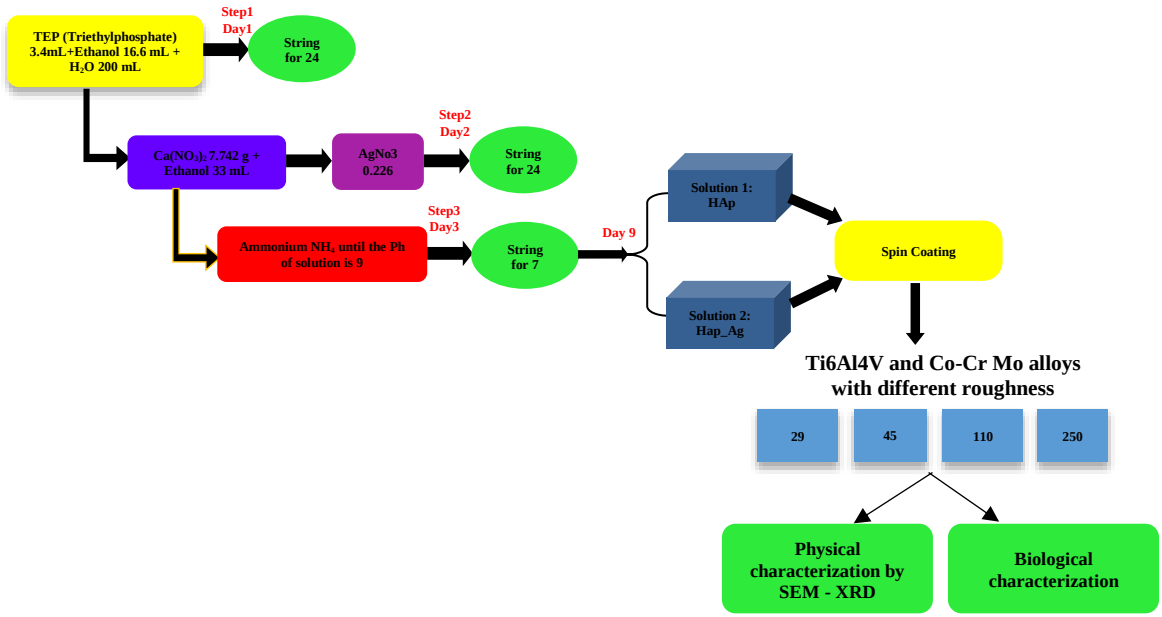

Fig. 3.1. Shows the technical flow to obtaining and characterization for surfaces of both alloys

3.1.2 Materials used

For thesis work, a plates of **Ti6Al4V** and **Co-Cr-Mo** alloys were used, with dimensions about 5x5 mm with thicknesses of 2 and 0.5 mm respectively, after the required surface treatment has been performed, these plates were processed by using blasting process with different particles sizes (29 µm, 45 µm, 110 µm, 250 µm) to produced different surface roughness for each samples, after that, the both of sample types were coated with hydroxyapatite doped and undoped silver by spin-coating technique using Spin Coater from Laurell model WS-650 device.

3.1.3 Spin coating

The starting materials used in this process contain spin coater machine, specimens of **Ti6Al4V** alloys with different roughness of specimens obtained by sand blasting then polished **Ti6Al4V** alloys with steel balls of 29 um ,45 um, 110 um , and 250 um , we issue that the roughness is proportion with the size of levels used, ScanTemp 490 Infrared thermometer and heating magnetic stirrer.

The samples of **Ti6Al4V** and **Co-Cr-Mo** alloys were coated with 20 thin layers of doped and undoped phosphatic ceramic HAp, by using Spin Coater from Laurell model WS-650 at a speed of 2000 rpm for 5 seconds., the films were dried at 80 °C for 10 min after every deposited layer.

Finally the samples heat treated at 500 °C for 30 min in order to assure a suitable roughness benefic for an advanced adherence which applied for all surfaces covered with thin films. As well as the analysis will conduct subsequently.

The sample code of **Ti6Al4V** and **Co-Cr-Mo** alloys coated by hydroxyapatite doped and undoped silver shown in ***table 3.1***

Table 3.1. shows the code of Ti6Al4V and Co-Cr-Mo alloy coated by silver doped and undoped HAp

Code	alloy	Code	alloy	Blasting balls of different sizes (µm)	Layer deposited
HAp_29 ^{Ti}	**Ti6Al4V**	**HAp_29^{Co}**	**Co-Cr-Mo**	**29**	**Hydroxyapatite**
HAp_45 ^{Ti}	**Ti6Al4V**	**HAp_45^{Co}**	**Co-Cr-Mo**	**45**	**Hydroxyapatite**
HAp_110 ^{Ti}	**Ti6Al4V**	**HAp_110^{Co}**	**Co-Cr-Mo**	**110**	**Hydroxyapatite**
HAp_250 ^{Ti}	**Ti6Al4V**	**HAp_250^{Co}**	**Co-Cr-Mo**	**250**	**Hydroxyapatite**
HAp_Ag_29 ^{Ti}	**Ti6Al4V**	**HAp_Ag_29^{Co}**	**Co-Cr-Mo**	**29**	**Hydroxyapatite _Silver**
HAp_Ag_45 ^{Ti}	**Ti6Al4V**	**HAp_Ag_45^{Co}**	**Co-Cr-Mo**	**45**	**Hydroxyapatite _ Silver**
HAp_Ag_110 ^{Ti}	**Ti6Al4V**	**HAp_Ag_110^{Co}**	**Co-Cr-Mo**	**110**	**Hydroxyapatite _ Silver**
HAp_Ag_250 ^{Ti}	**Ti6Al4V**	**HAp_Ag_250^{Co}**	**Co-Cr-Mo**	**250**	**Hydroxyapatite _ Silver**

3.1.4 Analysis and characterization techniques

The obitaine samples were analyzed by advanced characterization techniques:

3.1.4.1. X-ray diffraction (XRD)
3.1.4.2. Scanning Electronic Microscopy (SEM)
3.1.4.3. Film stability in the Simulated Body Fluid (SBF)
3.1.4.4. Biological characterization

CHAPTER 4: RESULTS AND DISCUSION

A. (Ti6Al4V alloy)

A.4.1. X-ray Spectra (XRD)

A.4.1.1. Ti6Al4V alloys substrate.

Ti6Al4V can be observed by analyzing the spectra for the sample uncoated, that the sample of Titanium alloy Ti6Al4V without any Hap implantation obviously has the peaks which all attributed to α phase titanium, and there is no β phase diffraction peak in the alloy as shown in ***figure 4.1.***

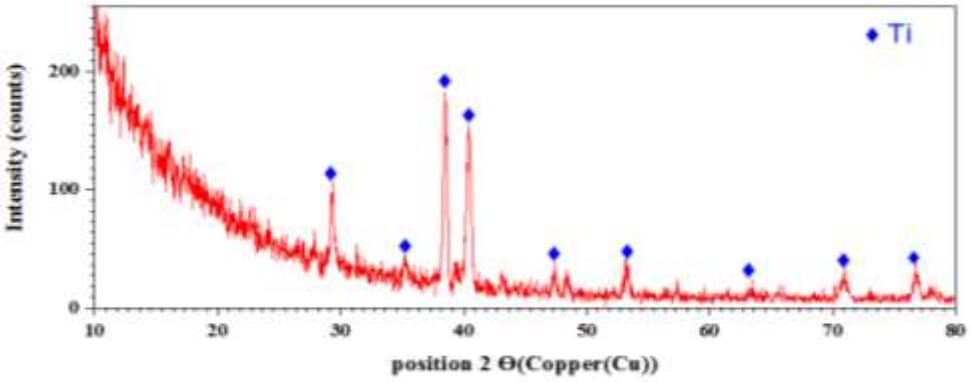

Fig. 4.1. shows the X-ray Spectra registered for the Ti alloy sample

A.4.1.2. HAp_29^{Ti}-HAp_45 ^{Ti} and HAp_110 ^{Ti} - HAp_ 250 ^{Ti}

In ***figures 4.2.*** the X-ray diffraction spectra of HAp_29^{Ti}-HAp_45 ^{Ti} , HAp_110 ^{Ti} - HAp_250 ^{Ti} can be observed by analyzing the spectra for the samples without silver, samples of HAp_29^{Ti} and Hap_45^{Ti} with roughness obtained by using balls of 29µm and 45µm respectively, have a phosphorus ceramic film with a rhombohedral structure composed of β-tricalcium phosphate $Ca_3(PO_4)_2$ in the hexagonal setting according to ASTM sheets 04-010-0295.It should be noted that the samples are well crystallized in both cases but also that the intensity of diffraction lines for $Ca_3(PO_4)_2$ decreases with increased roughness which induced by the balls with 45 µm. This can be attributed to the fact that Tricalcium diphosphate (TCP) $Ca_3(PO_4)_2$ was formed in holes due to the larger size of the balls.

In the case of diffraction spectra obtained for HAp_110^{Ti} and HAp_250 ^{Ti}, it can be seen that samples exhibit lower crystallinity compared to HAp_29 ^{Ti} and HAp_45 ^{Ti}, which is demonstrated by the intensity of smaller high diffraction lines. Both XRD Spectra reveal that the layer obtained and analyzed for surface of titanium alloys is $Ca_5(PO_4)_3(OH)$, in this case hydroxyapatite Hap is formed according to ASTM datasheets 00-009-0432 with Hexagonal structure, indicating that deposition has been successful, also because of poor sensitivity and the presence of interfering effects from the substrate, XRD geometry is not useful for the study of thin, graded composition and multilayered thin films.

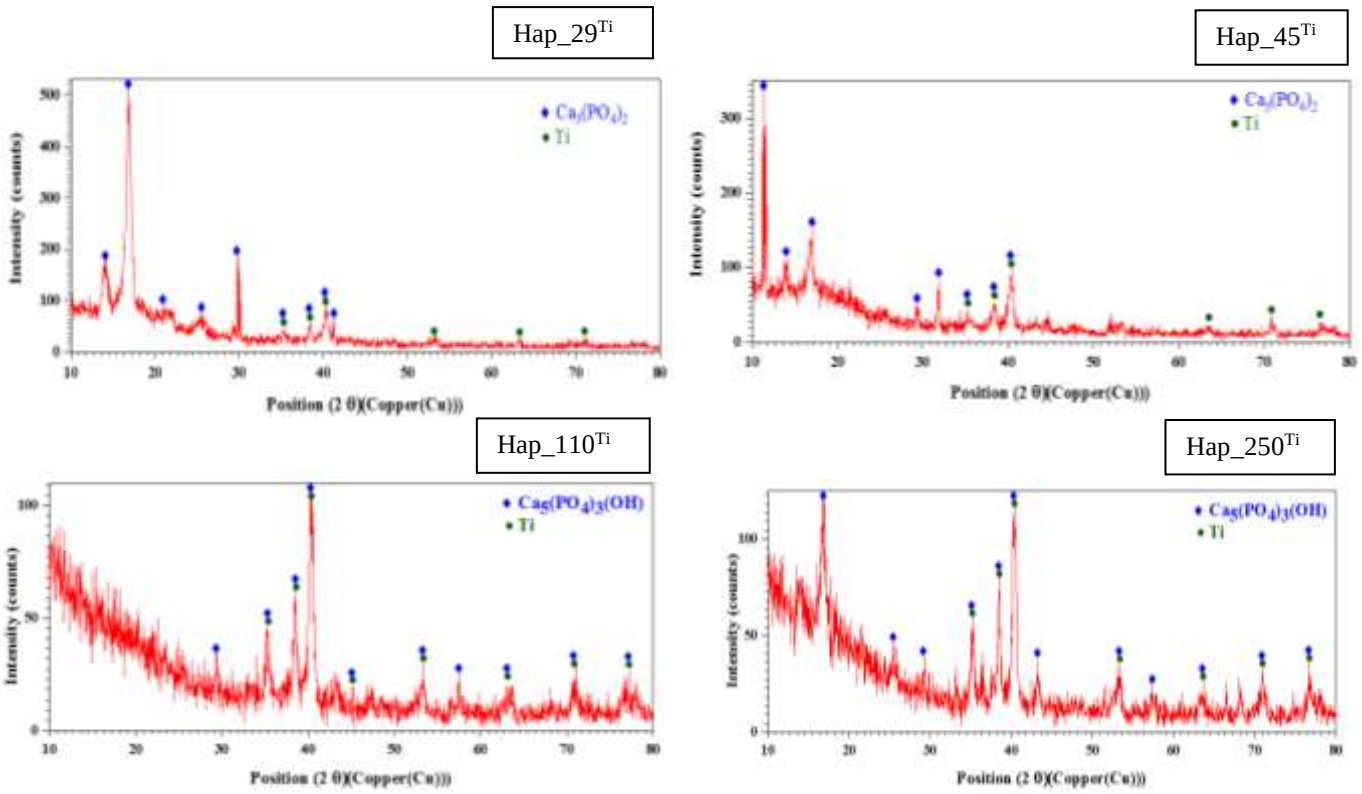

Fig 4.2. Shows the X-ray Spectra registered for the HAp_29^{Ti}-HAp_45 ^{Ti} and HAp_110 ^{Ti} - HAp_ 250 ^{Ti}

A.4.1.3. HAp_Ag_29^{Ti}-HAp_Ag_45 ^{Ti} and HAp_Ag_110 ^{Ti} - HAp_Ag_250 ^{Ti}

in ***figure 4.3.*** which shows the result observed a layer of phosphorus ceramic with a rhombohedral structure of Calcium Phosphate β-$Ca_3(PO_4)_2$ according to ASTM sheets 04-010-0295 for HAp_Ag_45^{Ti} while Tetragonal structure of Calcium Phosphate, Calcium diphosphate $Ca_2(P_2O_7)$ for HAp_Ag_29 ^{Ti} according to ASTM sheets 04-009-6231. the difference in crystallinity which is noted higher for HAp_Ag_29 ^{Ti} where the roughness was obtained with 29µm balls than the sample HAp_Ag_45 ^{Ti}.

For samples HAp_Ag_110^{Ti} and HAp_Ag_250 ^{Ti}, where the roughness is obtained with particles size 110µm and 250µm, the diffraction spectrum shows that the deposition was successful, and in both cases the hydroxyapatite with the hexangular structure of $Ca_5(PO_4)_3(OH)$. At the same time, the intensity of the diffraction lines supports the high crystallinity of the samples.

The titration according to the ASTM sheets 00-009-0432, which is used as a substrate for spin-coating deposition, is also found for diffractograms of analyzed samples.

By note identifying Ag+, it proofs that the Ag^+ is completely substituted by Ca^{+2} in the phosphate ceramics.

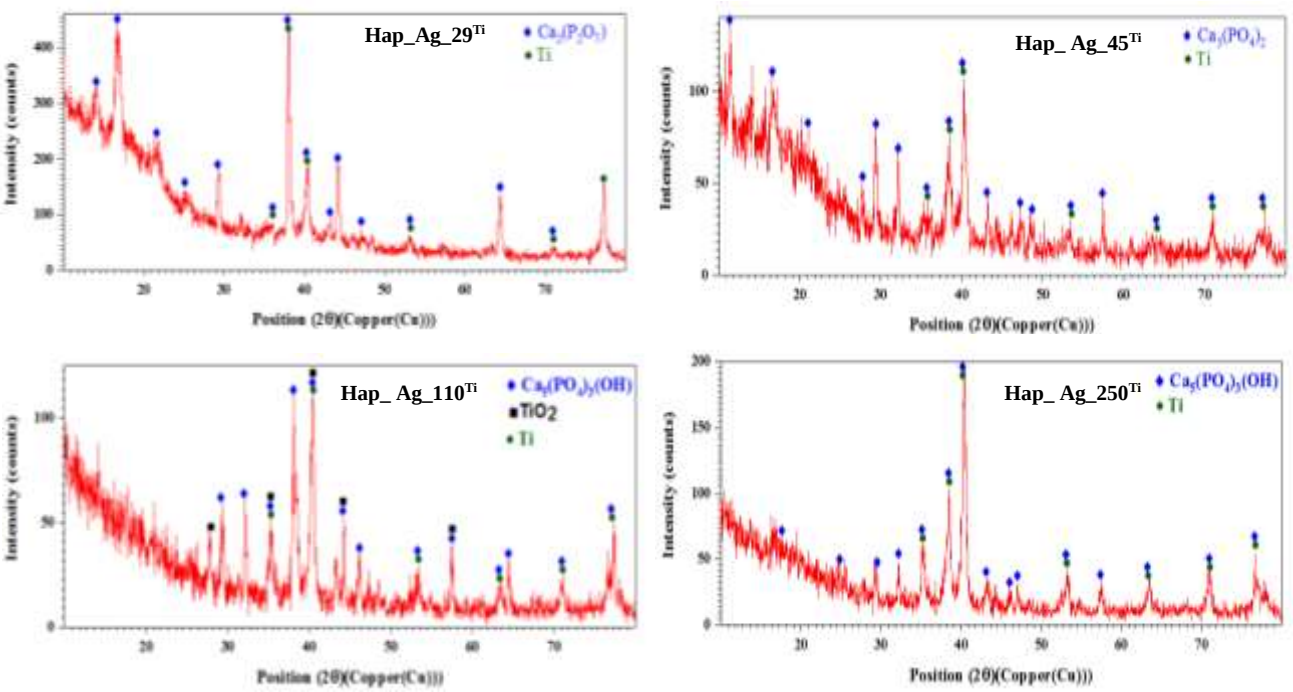

Fig. 4.3. Shows the X-ray Diffractogram registered for the HAp_Ag_29^{Ti}-HAp_Ag_45 ^{Ti} and HAp_Ag_110 ^{Ti} - HAp_Ag_250 ^{Ti}

A.4.2. Scanning Electron Microscopy (SEM)

Electronic Scanning Microscopy (SEM) is an investigative method that can provide relevant information about the structure and state of the material surfaces. it was used to investigate the morphological characteristics of hydroxyapatite doped and undoped silver, as a film deposited on the surface of the **Ti6Al4V** alloys.

A.4.2.1. Ti6Al4V alloys substrate.

It is noted in ***figure 4.4.*** the morphology of surfaces with different roughness of titanium alloys used as a substrate for the deposition of thin films of hydroxyapatite and silver doped hydroxyapatite.it observed clearly the roughness of the **Ti6Al4V** samples increases with the increase of particles size 19, 49, 110, and 250 µm during grit blasting process.

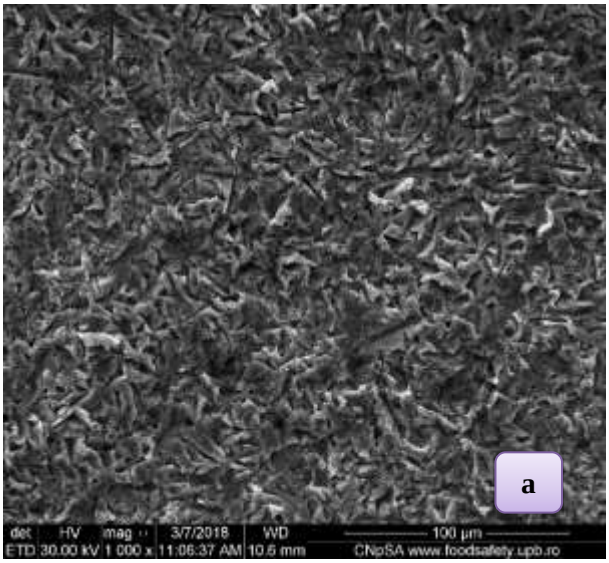

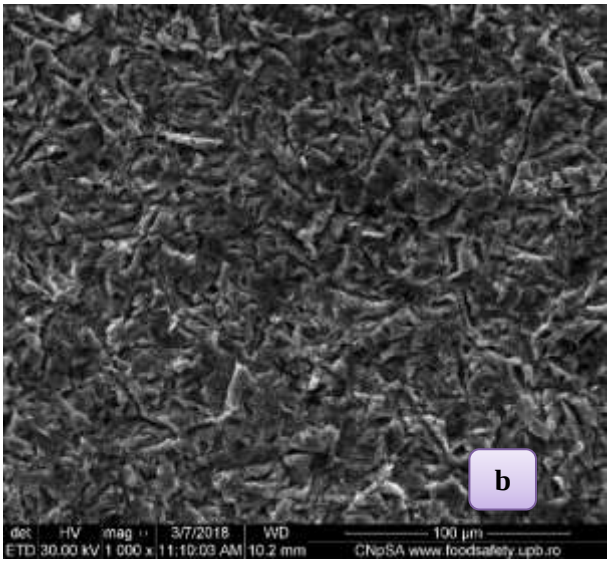

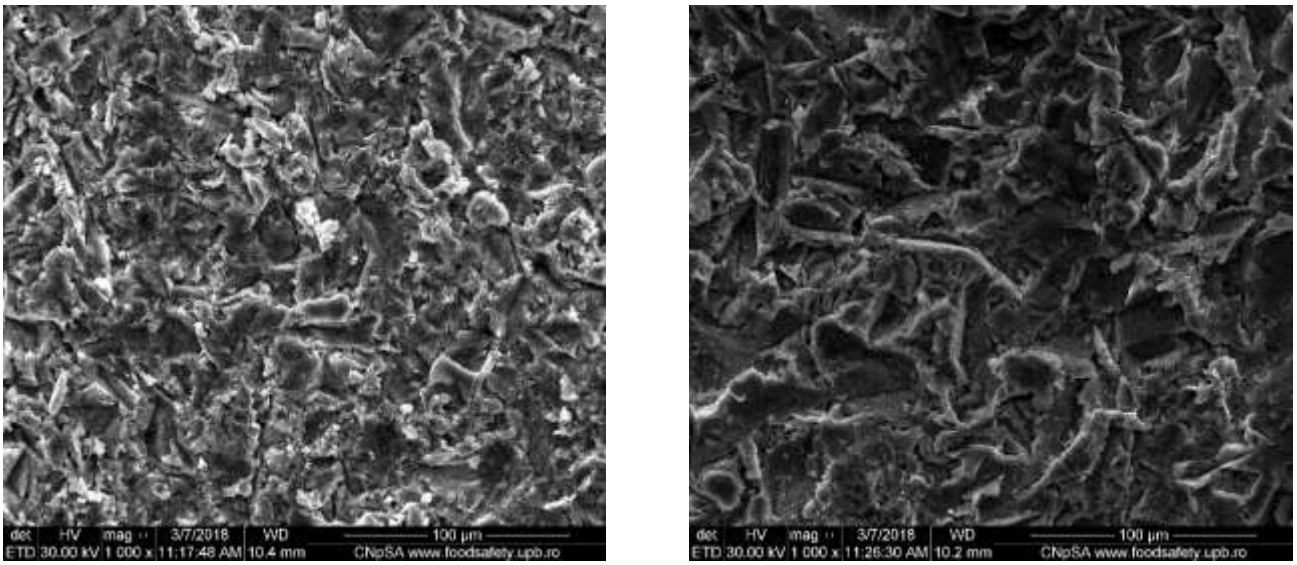

Fig. 4.4. Shows the SEM micrographs registered of Ti6Al4V substrate.with different roughness depending on particles size: a) 29 µm, b) 45 µm, c) 110 µm, d) 250 µm.

A.4.2.2. HAp_29 ^{Ti}, HAp_45 ^{Ti}, HAp_110 ^{Ti}, HAp_250 ^{Ti}.

it observed for the micrographs obtained of samples HAp_29^{Ti}, HAp_45^{Ti}, HAp_110^{Ti}, HAp_250^{Ti} that the deposited layer on the surface of Ti6Al4V alloy support is uniform, which is distributed in all the recesses formed by balls halls of different sizes 29, 45, 110, 250 µm.

For the samples HAp_110^{Ti} and HAp_250^{Ti}, the deposition of hydroxyapatite layer morphology presents polyhedral forms, because in this case HAp is not formed the structure of $Ca(PO_4)_2OH$.

The analysis of EDXS (Mapping) for HAp coated of differnet roughness surfaces of Ti6Al4V alloy samples confirms that the phosphate ceramic layers which have been deposited using the spin coating method , which have a uniform distribution of calcium, phosphorus and oxygen , so it s characteristic of the solution submitted as shown in ***figure 4.5***.

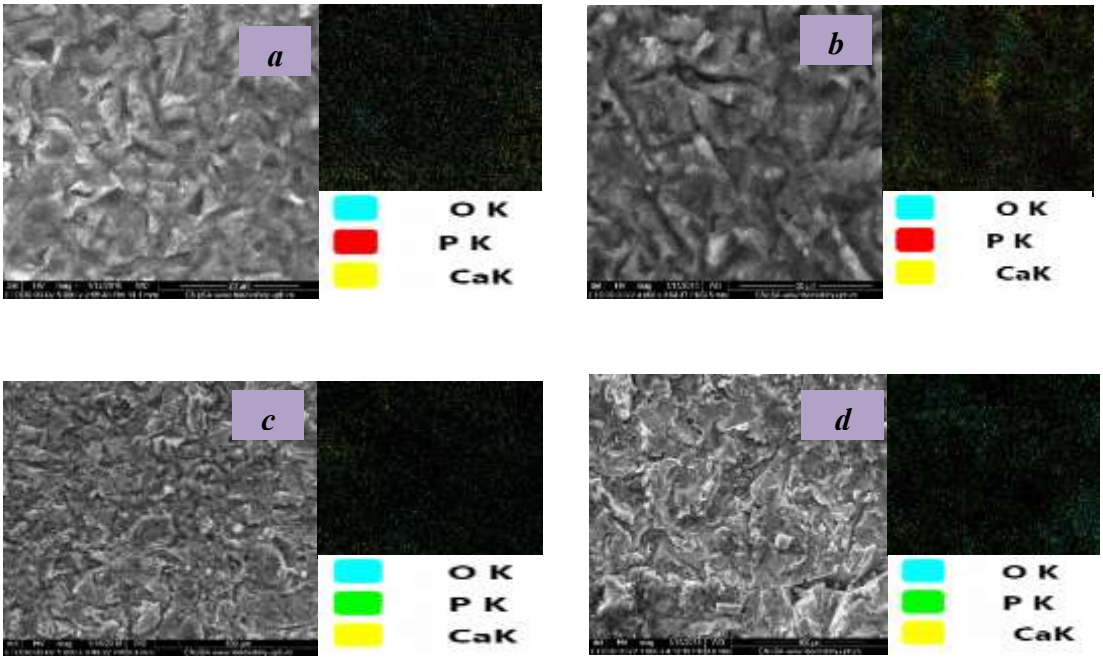

Fig.4.5. shows the SEM micrographs and mapping registered for sample a) Hap_29 ^{Ti}, b) Hap_45 ^{Ti},C) Hap_110 ^{Ti}, d)Hap_250 ^{Ti}

A.4.2.3 Hap_Ag_29^{Ti}, Hap_Ag_45^{Ti}, Hap_Ag_110^{Ti}, Hap_Ag_250^{Ti}.

In ***figure 4.6.*** the samples of HAp doped silver, coated a different roughness surfaces of Ti6Al4V alloy containing a silver as antibacterial agent in combination with hydroxyapatite, where that analysis of SEM micrographs demonstrate that the layer formed homogeneously a particles morphologies arranged on the surface of Ti6Al4V alloy support.

Moreover, the samples HAp_Ag-29^{Ti} and 45^{Ti} showed, it appears that an ordered abundance of the particulate solution of the deposited layer.

The results of EDXS (Mapping) analysis showed for each sample, that the precipitating layer is homogeneous , it be formed through the uniform distribution of specific elements such as calcium, phosphorus, oxygen and silver.

The samples HAp_Ag_110^{Ti} and 250^{Ti} contain almost equal proportions of calcium and silver, that represents a successful depositionas weel as, it can be concluded that the character of roughness directly influences on the deposition.sowhich means the deposition take place more successful.

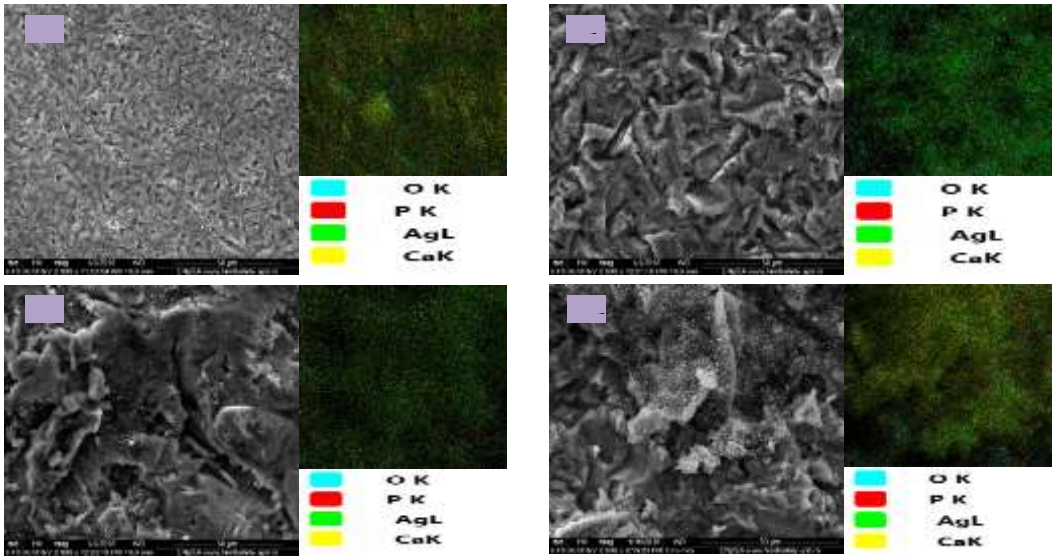

Fig.4.6. shoes the SEM micrographs and mapping registered for sample a) HAp_Ag_29 ^{Ti}, b) HAp_Ag_45 ^{Ti},C) HAp_Ag_110 ^{Ti}, d)HAp_Ag_250 ^{Ti}

A.4.3. Stabilization of thin films in SBF after 7, 14, and 21 days of immersion in SBF

The method of coating with HAp doped and undoped Silver can be based on practical bio-mimicry by immersing implants in the simulated body fluid (SBF), which is an equal inorganic composition with the pH and temperature of the human blood plasma.

The surface morphology of the spinning coated specimens was observed by a field scanning electron microscope SEM and X-ray spectra (XRD) analysis.

A.4.3.1. X-ray Diffraction Analysis

A.4.3.1.1. HAp_29^{Ti}, HAp_45 ^{Ti}, HAp_110^{Ti}, HAp_250^{Ti}

In ***figure 4.7.*** it can beobserved that the X-ray spectra of HAp_29^{Ti} - HAp_250^{Ti} for 7 days , can be observed by analyzing the spectra for the samples without silver, that samples of HAp_29^{Ti} and HAp_45 ^{Ti} with roughness obtained by using particle size of 29µm and 45µm respectively have a phosphorus ceramic film with Monoclinic crystal of calcium phosphate hydrate $Ca_2(P_4O_{12})_4H_2O$ and calcium phosphate $Ca(PO_3)_2$ but with HAp_29^{Ti}, it crystallized with calcium phosphate hydroxide $Ca_5(PO_4)_3(OH)$, than HAp_45 ^{Ti} for intensity of diffraction lines for $(Ca_2(P_4O_{12})_4H_2O$ decreases with increased roughness .

It can be also observed that, HAp_110^{Ti} and HAp_250^{Ti}, show a lower crystallinity compared to HAp_29^{Ti} and HAp_45 ^{Ti}, which is demonstrated by the intensity of smaller high diffraction lines, Both XRD Spectra reveal that the layer obtained and analyzed for surface of titanium alloys is $Ca_5(PO_4)_3(OH)$, in this case hydroxyapatite HAp is formed according to ASTM datasheets 00-

009-0432 with Hexagonal structure, indicating that stabilization of film has been good Apatite $Ca_5(PO_4)_3(OH)$, has long been considered as an excellent biomaterial to promote bone repairs and implant.

While after 14 days of immersion in SBF. That a family apatite are particularly evident during the immersion in SBF, when the roughness surfaces increased, the apatite structures increased.

But after 21 days of immersion in SBF. It be noted that structre of $Ca[PHO_3][H_2O]$ formed at the roughness HAp_29^{Ti}, HAp_45^{Ti} and HAp_250^{Ti} when immersion in SBF after 21 days , while HAp_45^{Ti} formed a structures of apatite family contains hexagonal structure of $Ca_5(PO_4)_2OH$ as hydroxyapatite and monoclinic crystal structure of $Ca(PO_3)_2$.

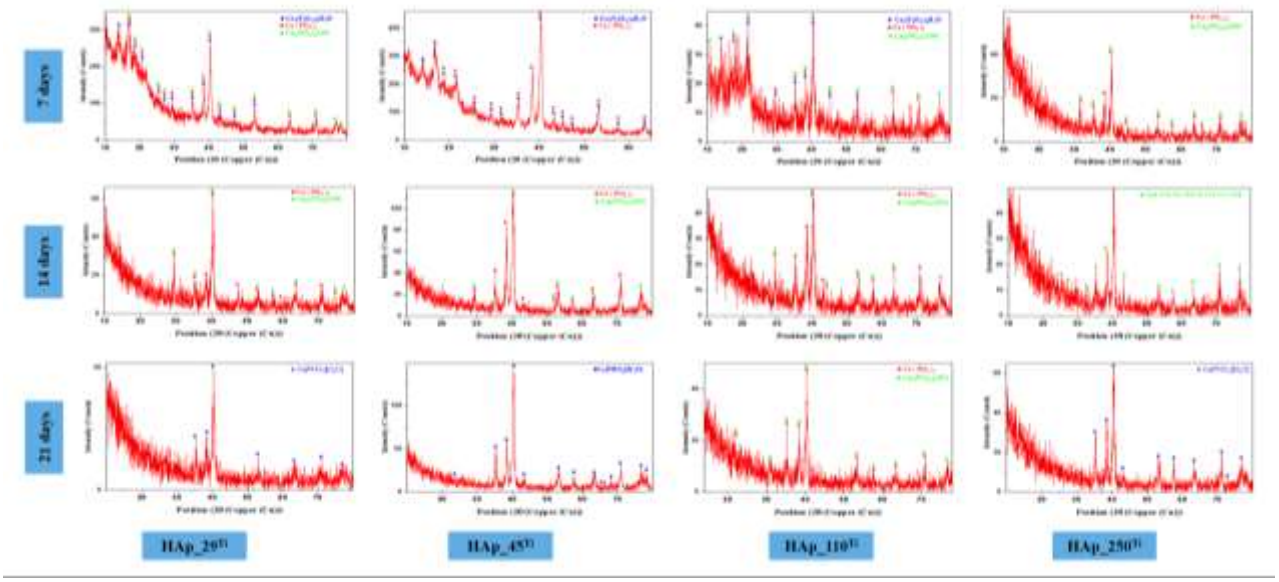

Fig 4.7. shows the X-ray Diffraction Analysis of samples HAp_29^{Ti}, HAp_45^{Ti}, HAp_110^{Ti}, HAp_250^{Ti} after 7, 14 and 21 days of immersion in SBF.

A.4.3.1.2. $HAp\_Ag\_29^{Ti}$, $HAp\_Ag\_45^{Ti}$, $HAp\_Ag\_110^{Ti}$, $HAp\_Ag\_250^{Ti}$

In ***figure 4.8*** it can be observed that the samples of silver doped HAp which are contain $HAp\_Ag\_29^{Ti}$ and $HAp\_Ag\_45^{Ti}$, also subjected to X-ray spectra analysis aster 7 days of immersion, The result of $HAp\_Ag\_29^{Ti}$ observed a layer of phosphorus ceramic with a hexagonal structure of calcium phosphate hydroxide $Ca_5(PO_4)_3(OH)$ according to ASTM sheets 00-009-0432, and monoclinic crystal structure of calcium phosphate $Ca(PO_3)_2$ according to ASTM sheets 00-050-0584, while $HAp\_Ag\_45^{Ti}$ contain calcium Phosphate $Ca(PO_3)_2$, and calcium Phosphate Hydrate $Ca_2(P_4O_{12})_4H_2O$ as monoclinic crystal structure according to ASTM sheets 00-041-0483.as well as, a structure of calcium phosphate hydroxide within apatite family $Ca_{4.65}(PO_4)_3(OH)_{0.3}(H_2O)$ [74] of high crystallinity of the samples.

For samples HAp_Ag_110Ti and HAp_Ag_250Ti , the diffraction spectrum shows that the stabilization was successful, with a structures of apatite family which contain calcium Phosphate Hydrate as monoclinic structure of $Ca_2(P_4O_{12})\cdot 4H_2O$ according to ASTM sheets 00-041-0483 and calcium phosphate $Ca(PO_3)_2$ in addition to $Ca_{4.626}(H_{0.588}(PO_4)_3(OH)_{0.84}$ as a one structure of apatite family. At the same time, the intensity of the diffraction lines supports the high crystallinity of the samples.

While 14 days of immersion , The result of $HAp\_Ag\_29^{Ti}$ observed a layer of phosphorus ceramic with a hexagonal structure of calcium phosphate hydroxide $Ca_5(PO_4)_3(OH)$ according to ASTM sheets 00-009-0432, and monoclinic crystal structure of calcium phosphate $Ca(PO_3)_2$ according to ASTM sheets 00-050-0584, while $HAp\_Ag\_45^{Ti}$ contain calcium Phosphate $Ca(PO_3)_2$, and calcium Phosphate Hydrate $Ca_2(P_4O_{12})_4H_2O$ as monoclinic crystal structure according to ASTM sheets 00-041-0483.as well as, a structure of calcium phosphate hydroxide

within apatite family $Ca_{4.65}(PO_4)_3(OH)_{0.3}(H_2O)$ [74] of high crystallinity of the samples.

For samples HAp_Ag_110^{Ti} and HAp_Ag_250^{Ti} , the diffraction spectrum shows that the stabilization was successful, with a structures of apatite family which contain calcium Phosphate Hydrate as monoclinic structure of $Ca_2(P_4O_{12})\cdot 4H_2O$ according to ASTM sheets 00-041-0483 and calcium phosphate $Ca(PO_3)_2$ in addition to $Ca_{4.626}(H_{0.588}(PO_4)_3(OH)_{0.84}$ as a one structure of apatite family. At the same time, the intensity of the diffraction lines supports the high crystallinity of the samples.

It noted that for each surface roughness of Ti6Al4V coated by hydroxyapatite, HAp growth increased with increasing the time of immersion indicated by HAp peaks. Therefore the film formed converted to more stable when immersed after 21 days in SBF especially with HAp_250^{Ti} and HAp_Ag_250^{Ti}.

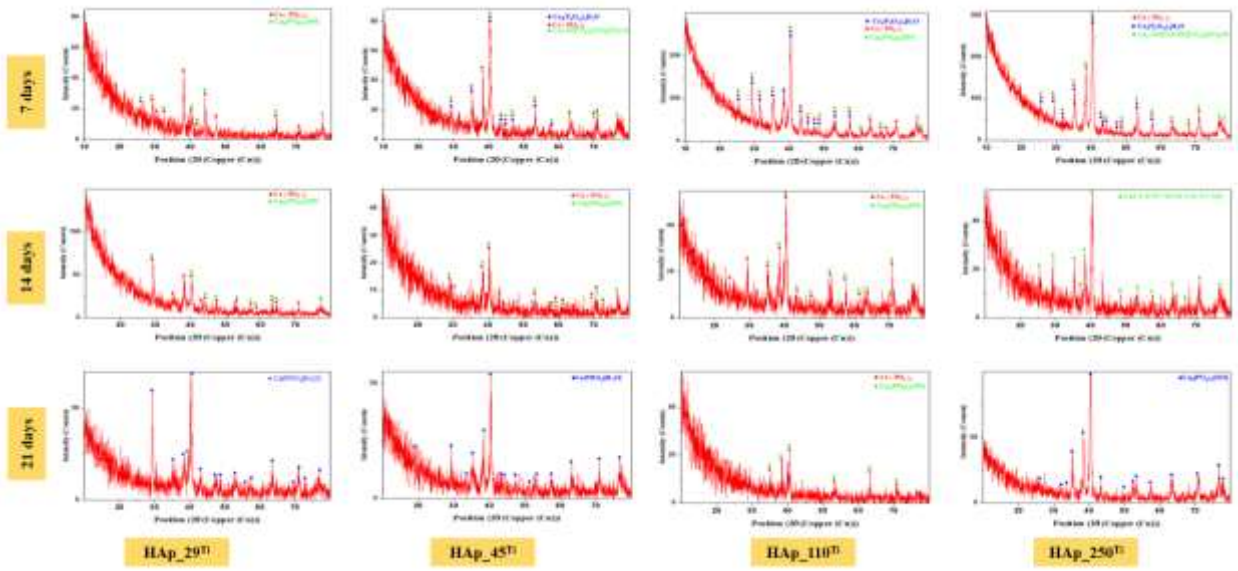

Fig 4.8. shows X-ray Diffraction Analysis of samples HAp_Ag_29^{Ti}, HAp_Ag_45^{Ti}, HAp_Ag_110^{Ti,} HAp_Ag_250^{Ti} after 7, 14 and 21 days of immersion in SBF.

A.4.3.2. Scanning Electron Microscope (SEM)

A.4.3.2.1 HAp_29^{Ti}, HAp_45^{Ti}, HAp_110^{Ti}, HAp_250^{Ti}

The ***figure 4.9.*** which provide the scanning electron microscopy of HAp_29^{Ti}, HAp_45^{Ti}, HAp_110^{Ti}, HAp_250^{Ti} after 7,14 and 21 days of immersion in SBF.

Depending on SEM micrographs which performed after 7 days immersion in SBF, it can be noted according to the figure above 4.35. That the phosphatic ceramic film has developed quantitatively at the same time of presenting a homogeneous arrangement on the surface of the titanium alloys. This is an indication of high activity of hydroxyapatite in contact with physiological fluid in the human body. By comparison, it can be consider that HAp_110^{Ti} shows the best development of the formed film, so the roughness is directly involved in the stability of thin films.

According to SEM micrographs obtained after 14 days of immersion in SBF, it can be noted that the phosphate ceramic film has a more significant development on the surface of Ti6Al4V alloy substrate than the micrographs obtained 7 days after immersion.

The success of HAp film deposition on roughness surfaces of Ti6Al4V alloy due to growth of hydroxyapatite homogeneously and constantly on surfaces of Ti6Al4V alloy, But it so observed to be agglomerated after 21 days of immersion in SBF.

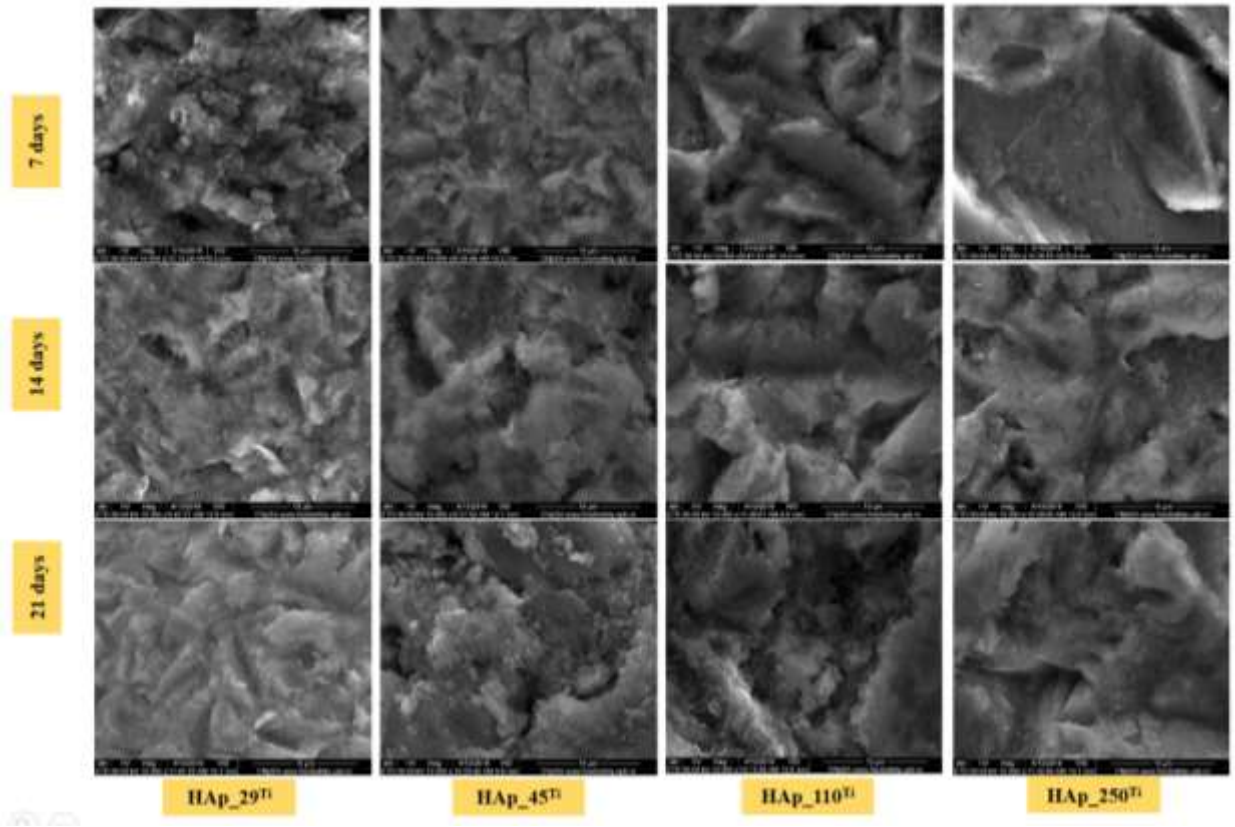

Fig. 4.9. shows the scanning electron microscopy of HAp_29Ti, HAp_45Ti, HAp_110Ti, HAp_250Ti after 7,14 and 21 days of immersion in SBF

A.4.3.2.2 HAp_Ag_29^{Ti}, HAp_Ag_45^{Ti}, HAp_Ag_110^{Ti,} HAp_Ag_250^{Ti}

The ***figure 4.10.*** which provide the scanning electron microscopy of HAp_Ag_29^{Ti}, HAp_Ag _45^{Ti}, HAp_Ag _110^{Ti}, HAp_Ag _250^{Ti} after 7, 14 and 21 days of immersion in SBF.

The samples of HAp doped with antibacterial agent (silver), it is observed that after 7 days of immersion in SBF, the film of phosphatic ceramic grows significantly on all roughness surfaces of Ti6Al4V alloy substrate.

The silver particles of samples HAp_Ag_29^{Ti} and HAp_Ag_250^{Ti} are arranged in the form of agglomerations in locations remote from each other. It noted that silver is not identified of HAp_Ag_45^{Ti} and HAp_Ag_110^{Ti}, which is correlated with its release into the SBF solution "because growth of the thickness of film in SBF.

The deposited film in SBF acts as nucleation growth, thus phosphate ceramic growth on the sample", thus, for the two samples still presenting silver particles it can be said that their antibacterial action is more developed compared to the other two samples where silver is not detected.

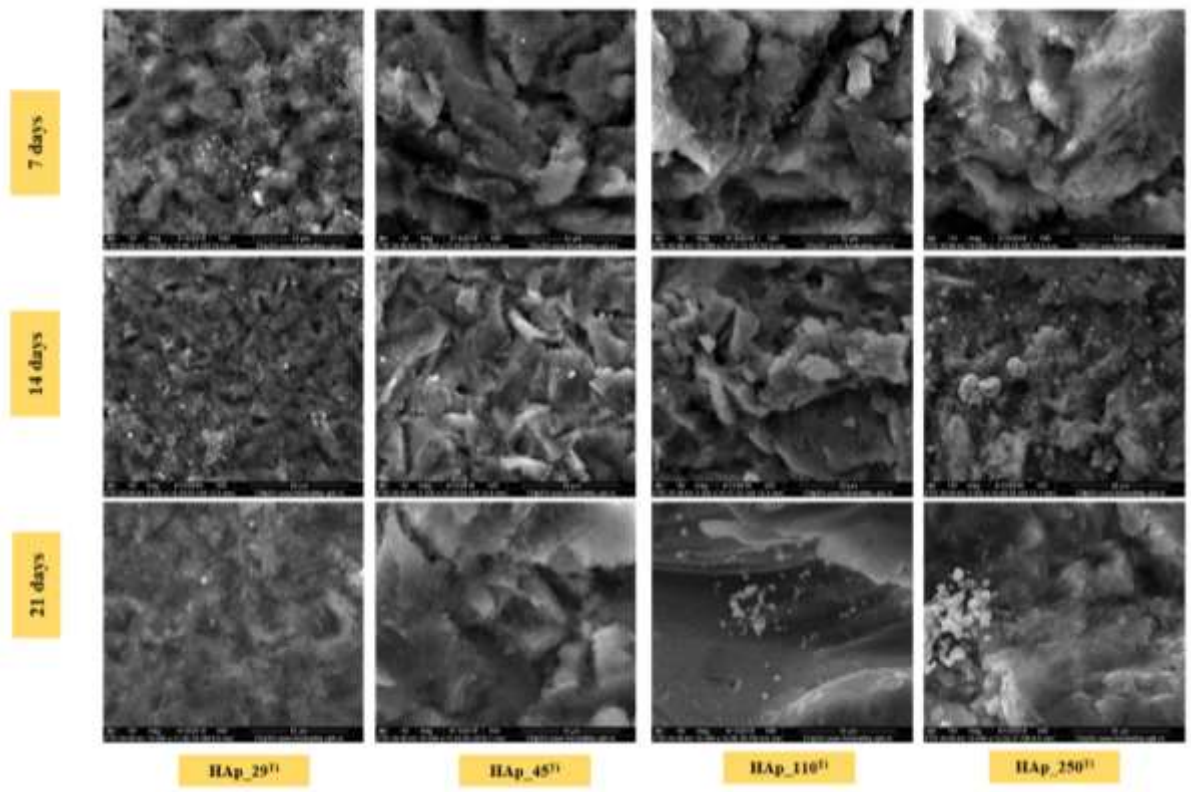

Fig. 4.10. shows the scanning electron microscopy of HAp_Ag_29^{Ti}, HAp_ Ag_45^{Ti}, HAp_ Ag_110^{Ti}, HAp_ Ag_250^{Ti} after 7,14 and 21 days of immersion in SBF

A.4.4. Biological characterization

The effect of the materials obtained on the growth of microorganisms in liquid media (planktonic cultures) by using *P.seudomonas aeruginosa* strain, and the effect of the surfaces obtained on the production of biofilms were tested , in order to establish the antimicrobial activity of Ti6Al4V alloys coated with hydroxyapatite doped and undoped silver. The samples of test have been encoded with numbering CODs as shown in ***table 4.1***. have also been taken during biological analysis as shown in ***figure 4.11.***

Table 4.1 CODs of samples of biological analysis

Code	**1**	**2**	**3**	**4**	**5**
Sample	HAp_Ag_29 ^{Ti}	HAp_Ag_45 ^{Ti}	HAp_Ag_110 ^{Ti}	HAp_Ag_250 ^{Ti}	HAp_29 ^{Ti}
Code	6	7	8	9	10
Sample	HAp_45 ^{Ti}	HAp_110 ^{Ti}	HAp_250 ^{Ti}	Ctrl	P.A CTRL

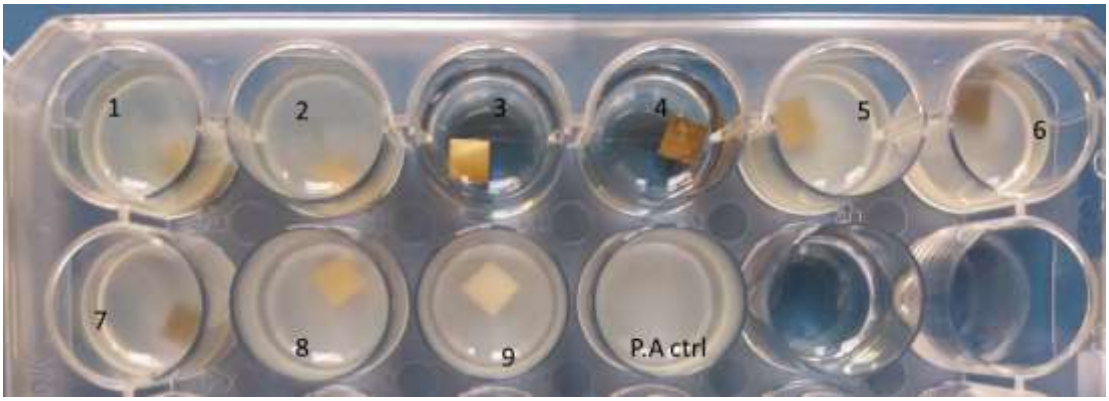

Fig. 4.11. Shows the samples during biological analysis by microbial cultures (P. aeruginosa)

A.4.4.1 Planktonic cultivation- bacterial growth in the presence of materials

For samples 3 and 4, there is no microbial growth was detected visually or spectrophotometrically, which demonstrates the high antimicrobial effect of the obtained materials.

When the spectrophotometric investigation completed, it can be seen from the graph that the samples have an inhibitory effect on bacterial action on the *P. aeruginosa* strain as shown in ***figure 4.12.*** $HAp\_Ag\_110^{Ti}$ and $HAp\_Ag\_250^{Ti}$, also its less notable of HAp_29^{Ti} and HAp_45^{Ti}, That means the roughness of the materials obtained by using size particles of 110 and 250 μm and silver ion, have a positively influences of the antibacterial activity for the samples on the *P. aeruginosa* strain. On the other hand, the samples of hydroxyapatite undoped silver as antibacterial agent have an inhibitory effect on bacterial action especially of HAp_110^{Ti} and HAp_250^{Ti} as a result of surface roughness formed antibiotic compounds of $Ca_5(PO_4)_3OH$ [75].

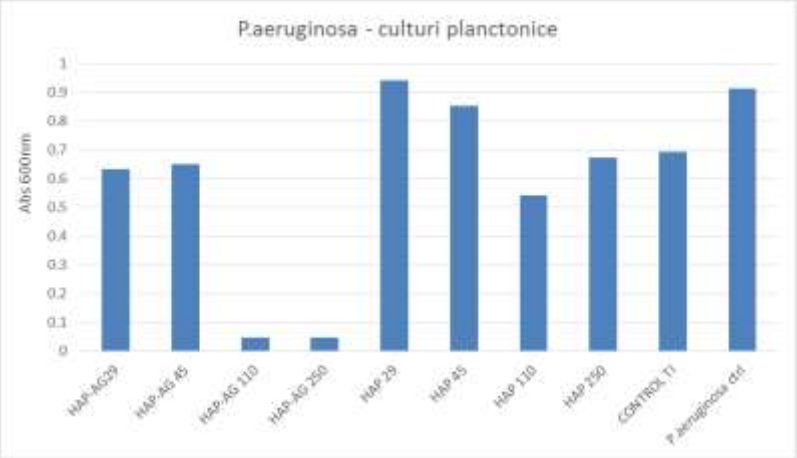

Fig. 4.12. Shows the Abs values at 600 nm suggesting the growth of planktonic microorganisms in the presence of Ti-based materials.

A.4.4.2. Investigation of biofilm formation on the samples obtained

Materials were analyzed to evaluate of biofilm formation , as well as, the samples were allowed to incubate for 24 hours and subsequently evaluated, It can be seen from the graph that all silver-containing samples showed some inhibitory effect on the formation of monospecific biofilms by P. aeruginosa species, the most significant inhibitory effects of their development being observed in samples 3 and 4, on the surface of which layers of hydroxyapatite with silver were deposited.

It can be noted from the ***figure 4.13***. some inhibitory effect being observed in samples 3 and 4 on the formation of monospecific biofilms by P. aeruginosa species, indicated to most significant effects of the high roughness of surface on hydroxyapatite coating which inhibitory of their development. While the samples 7 and 8 indicated of hydroxyapatite undoped silver as antibacterial agent have an a less activity than hydroxyapatite doped silver, on the other hand, it noted that the surface roughness has the direct effect on the production of biofilms , that s mean with increasing the roughness due to increase of production of biofilms as results of the compositions formed during coating which have that effections.

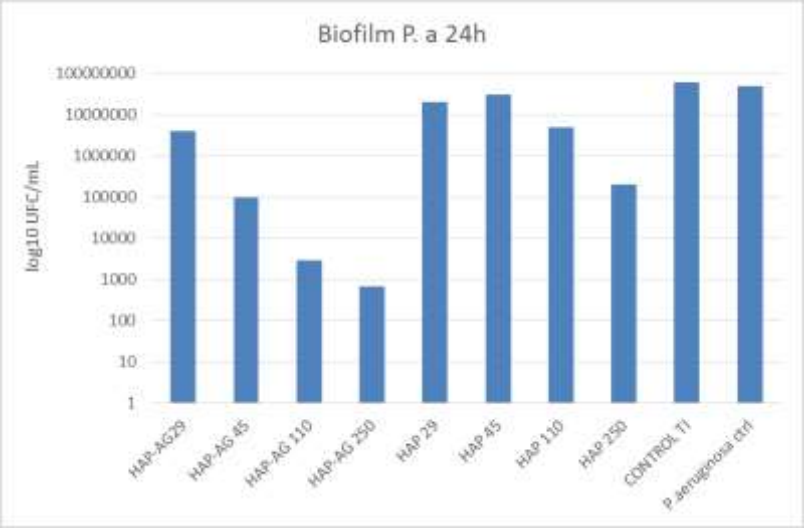

Fig. 4.13. Shows the graphical representation of UFC / mL values representing the development of biofilms on the tested surfaces.

B. (Co-Cr-Mo alloy)

B.4.1. X-ray Spectra (XRD)

B.4.1.1. HAp_29^{Co}-HAp_45 ^{Co} ,HAp_110 ^{Co} and HAp_ 250 ^{Co}

In ***Figure 4.14*** , it can be observed that analyzing of spectra for HAp 29^{Co} with roughness obtained by using balls of 29µm, has a precipitation of dicalcium phosphate (brushite) $CaHPO_4.2H_2O$ as film with the monoclinic crystal structure are very similar to those of gypsum [76]. But sample of HAp_45^{Co} with roughness obtained by using balls of 45µm, has Calcium Phosphide Ca_5P_8 film with monoclinic crystal structure according to ASTM sheets 00-048-1825. It should be noted that the samples are monoclinic crystallized in both cases but with different of crystals with increased roughness which induced by the balls with 45 µm, also Co and P as Hexagonal crystal structure noted according to ASTM sheets 04-015-9495 and 00-056-1217 respectively.

While for HAp_110^{Co} and HAp_250^{Co}, it can be seen that samples exhibit lower crystallinity compared to HAp_29^{Co} and HAp_45^{Co}, which is demonstrated by the intensity of smaller high diffraction lines. Both XRD Spectra reveal that the layer obtained and analyzed for surface of Co-Cr alloys is γ-$Ca_2P_2O_7$ as intermediate products for calcium phosphate of hydroxyapatite HAp formed according to ASTM datasheets 00-003-0605, indicating that deposition has been successful. It should be noted that the samples of HAp_110^{Co} contain chromium phosphate $Cr_2(P_2O_7)$ as oxide interlayer with monoclinic crystal structure according to ASTM datasheets 00-003-0605 , while HAp_250^{Co} contain to calcium phosphate $Ca_2P_2O_7$ and calcium chromium oxide $Ca_2Cr_2O_5$ as oxide interlayer with orthorhombic crystal structure according to ASTM datasheets 00-066-0840.

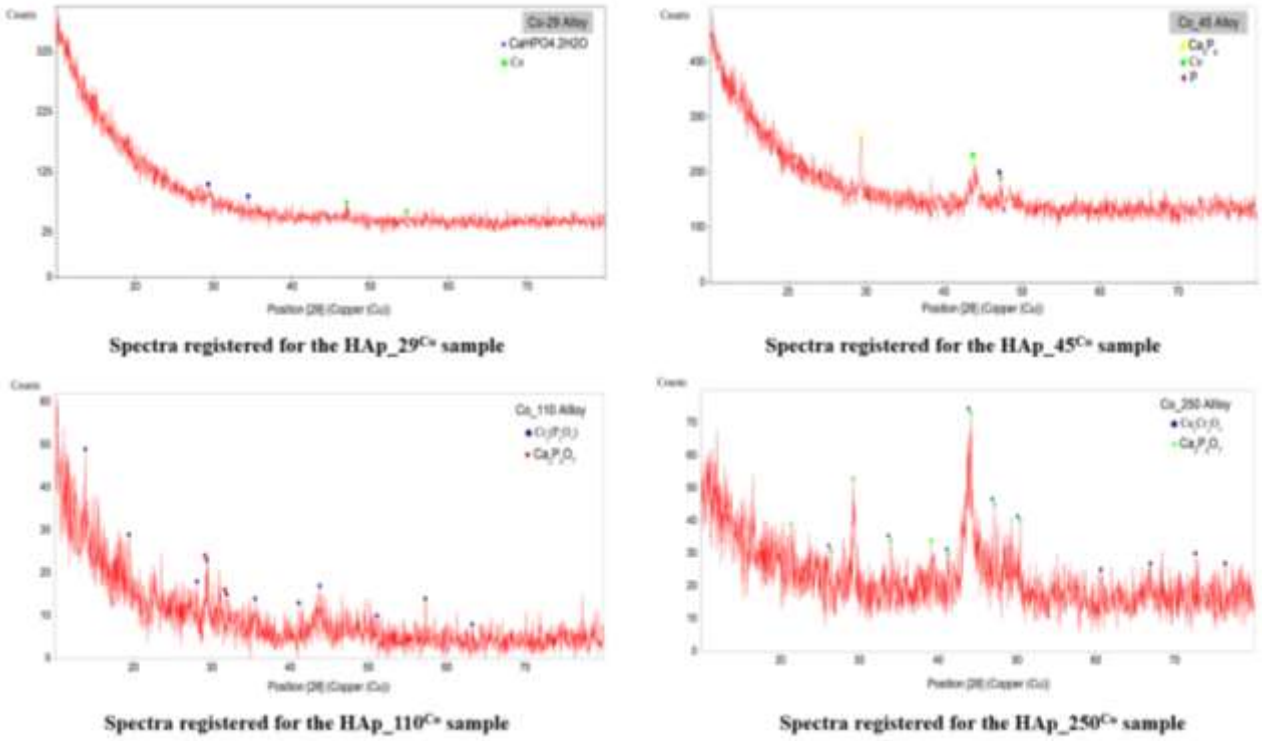

Fig. 4.14 Shows the X-ray Spectra registered for the silver undoped HAp_29^{Co}-HAp_45 ^{Co} ,HAp_110 ^{Co} and HAp_ 250 ^{Co}

B.4.1.2. HAp_Ag_29^{Co}-Hap_Ag_45 ^{Co} ,HAp_Ag_110 ^{Co} and HAp_Ag_ 250 ^{Co}

in ***figure 4.15***, it be noted from X-ray spectra analysis that a layer of calcium hydrogen phosphate which one of calcium phosphate compounds, thus helps to increase the bioactivity with an anorthic structure of monocalcium phosphate anhydrous (MCPA)$Ca(H_2PO_4)_2$ as slightly inferior solubility and similar properties to MCPM [77]; according to ASTM sheets 00-009-0390. While HAp_Ag_45^{Co} have a calcium pyrophosphate $Ca_2(P_2O_7)$ deposition according to ASTM sheets 00-003-0605. The difference in crystallinity which is noted higher for HAp_Ag_45^{Co} than HAp_Ag_29^{Co} where the roughness was obtained with particle size 45µm than the sample HAp_Ag_29^{Co}, due to the larger size of the particles. That the intensity of diffraction lines for $Ca(H_2PO_4)_2$ decreases with increased roughness which induced by the particles with 45 µm to form $Ca_2(P_2O_7)$.

Where the roughness is obtained with the help of the particles size 110µm and 250µm, the diffraction spectrum shows that hydroxyapatite undergoes incongruent melting and decomposes to tetracalcium phosphate as bioceramic with the tetragonal structure of Ca_4P_2O according to the ASTM sheets 04-010-2306, it means that water may be lost while crystallized the HAp structure. At the same time, the intensity of the diffraction lines supports the high crystallinity of the samples. While decomposition of HAp_Ag_250^{Co} to calcium pyrophosphate dihydrate (CPPD) with structure of β-$Ca_2P_2O_7.2H_2O$ according to the ASTM sheets 00-003-0605.

For more information that Ag^+ is completely substituted by ca $^{+2}$ in the phosphate of HAp_Ag_110^{Co} , while the ions Ca, Co, Cr, P and Ag were released of others HAp_Ag^{Co} with according to the ASTM sheets 01-080-3893, 04-015-9495, 04-007-2208, 00-056-1217 and 04-004-6436 sequentially.

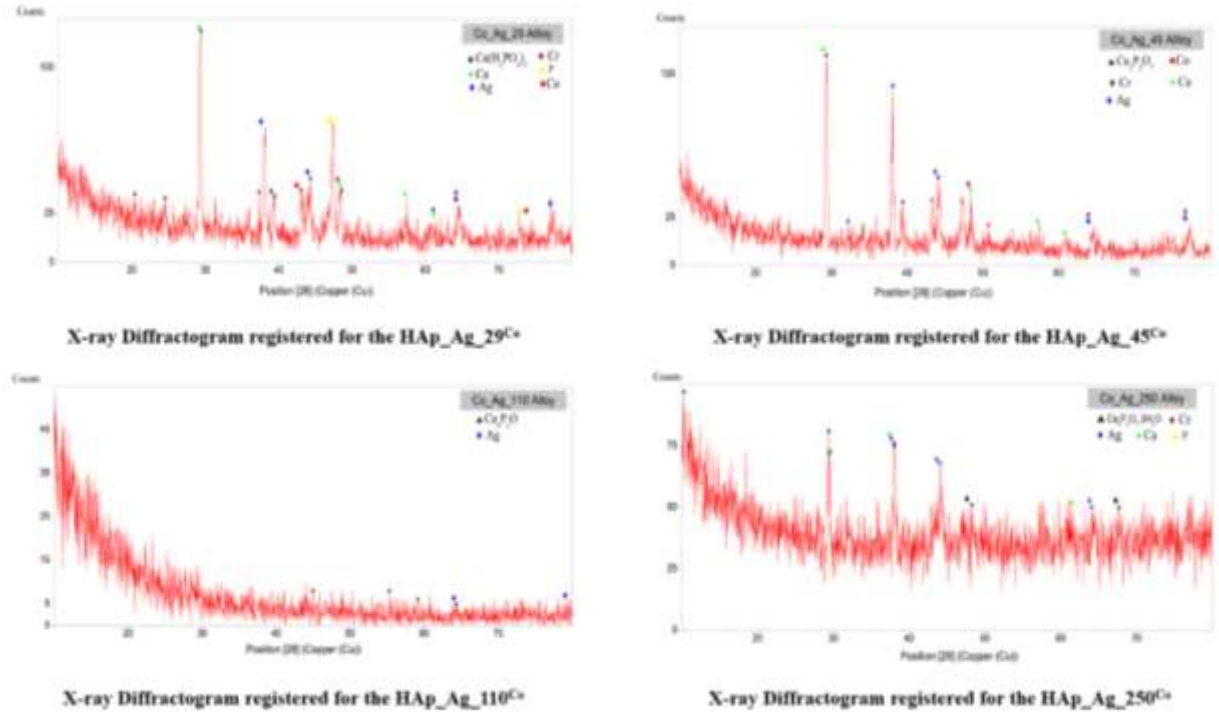

Fig. 4.15. Shows the X-ray Spectra registered for the silver HAp_Ag_29^{Co}-Hap_Ag_45 ^{Co} ,HAp_Ag_110 ^{Co} and HAp_Ag_ 250 ^{Co}

B.4.2. Scanning Electron Microscopy (SEM)

B.4.2.1. Co-Cr-Mo substrate alloy

In ***Figure 4.16***. which provide the SEM data of substrate for differnet roughness surfaces for Co-Cr-Mo alloy uncoated Hap, Shows the morphology of surfaces with different roughness of Co-Cr-Mo alloys used as a substrate for the deposition of thin films of hydroxyapatite doped and undoped silver. It can clearly see that; the roughness of the samples increases with the increases of particles size.

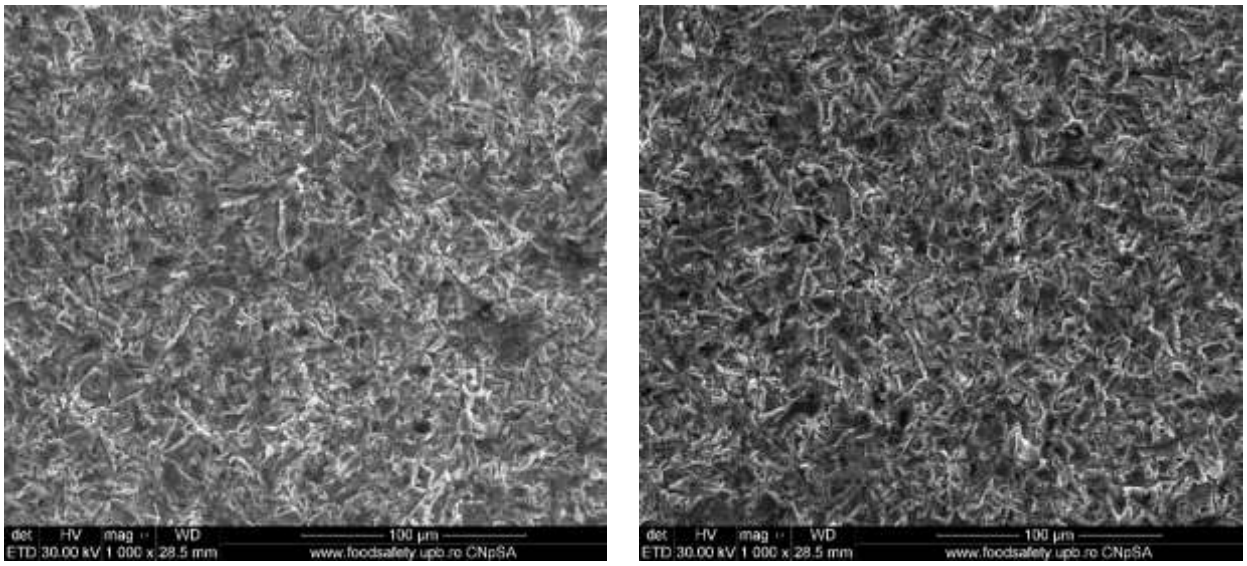

a) **b)**

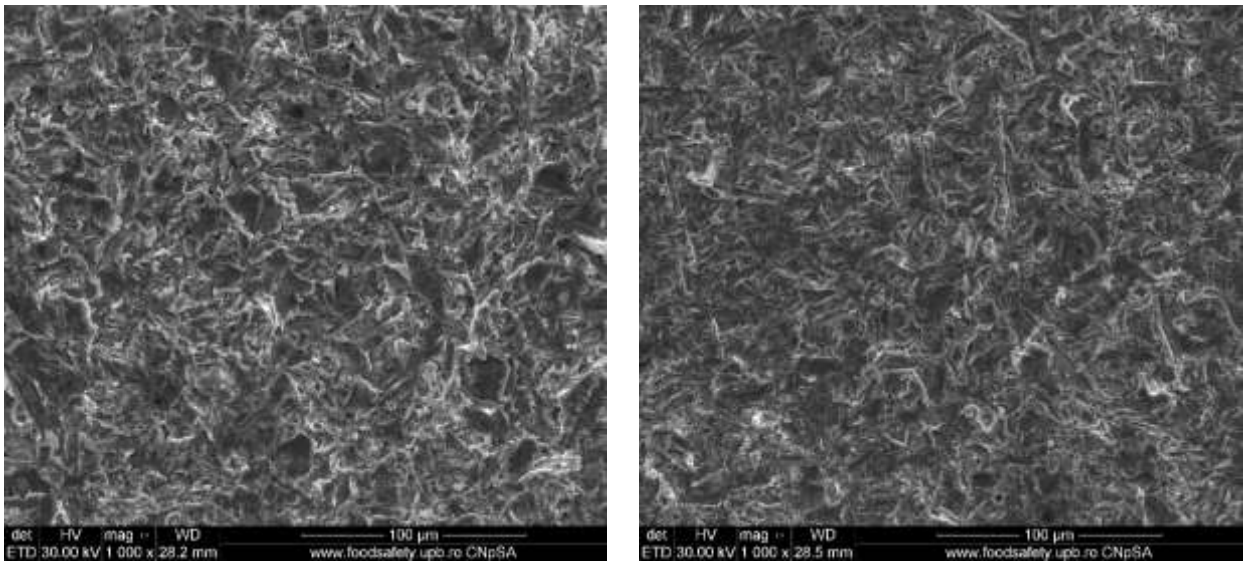

c) **d)**

Fig. 4.16 Shows the SEM micrographs registered of Co-Cr-Mo alloy substrates with roughness different obtained: a) 29 µm, b) 45 µm, c) 110 µm, d) 250 µm.

B.4.2.2. HAp_29^{Co}-HAp_45 ^{Co} ,HAp_110 ^{Co} and HAp_ 250 ^{Co}

In ***Figure 4.17*** , It can be observed that micrographs obtained of samples HAp_29^{Co}, HAp_45^{Co} HAp_110^{Co}, HAp_250^{Co} contain a uniform deposited layer on the surface of **Co-Cr-Mo** alloys, as result of hydroxyapatite decomposition to compounds of calcium phosphate which is distributed with different crystal structures in all the recesses formed by particles of different sizes (29, 45, 110, 250µm).

It can be seen polyhedral forms for layer morphology of hydroxyapatite deposition, for HAp_29^{Co} , it can be see the morphology of the starting dicalcium phosphate (brushite) similar to those of gypsum which formed by typical homogeneous crystals, whose XRD data were previously reported elsewhere. While HAp_45^{Co} contain a pentacalcium octaphosphate structure as calcium phosphateas, for HAp_110^{Co} contain γ-$Ca_2P_2O_7$ and $Cr_2(P_2O_7)$ shows spheroids morphology distributed in γ-$Ca_2P_2O_7$ as smaller crystallites are formed shown in figure for HAp_250^{Co} while for $Ca_2P_2O_7$ and $Ca_2Cr_2O_5$ as spheroids morphology. Whatever there were no marked differences in the distribution of cells on the top surface of samples from the different groups of particles sizes (29, 45, 110, 250µm).

EDAX analysis performed of **Co-Cr-Mo** alloy samples, with phosphate ceramic layers which have been deposited using the spin coating method simultaneously confirms the uniform distribution of the specific species found, such as aluminum, calcium, cobalt, chromium and molybdenum characteristic of the solution submitted.

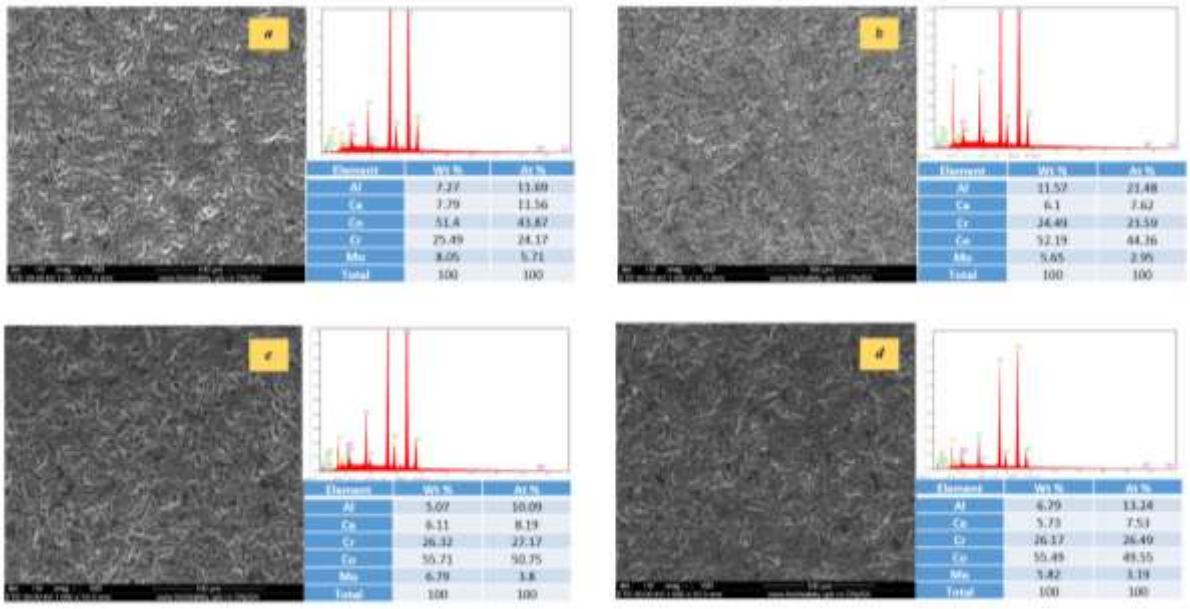

Fig. 4.17. The SEM micrographs and mapping registered for sample a) HAp_29 ^{Co}, b) HAp_45 ^{Co},C) HAp_110 ^{Co} , d)HAp_250 ^{Co}

B.4.1.2.3 HAp_Ag_29^{Co}-Hap_Ag_45 ^{Co} ,HAp_Ag_110 ^{Co} and HAp_Ag_ 250 ^{Co}

In ***figure 4.18.*** which provide the SEM data of samples HAp doped silver of coating differnet roughnes surfaces of Co-Cr-Mo. It can be observed that Samples containing the antibacterial agent silver in combination with hydroshows tyapatite, demonstrate in the SEM micrographs a layer showing particle morphologies homogeneously arranged on the surface of the **Co-Cr-Mo** alloy support. The samples HAp_Ag_29^{Co} and HAp_Ag_45^{Co} exhibit an ordered abundance of the particulate solution of the deposited layer. The results of the EDAX analysis of each sample confirm that the layer is homogeneously disposed of by the uniform distribution of specific elements such as calcium, cobalt, molybdenum, chromium, and silver. The samples HAp_Ag_110^{Co} and HAp_Ag_250^{Co} have roughly equal proportions of phosphor, calcium and silver, deposition being successful. Using micrographs, we can conclude that rugosity influences deposition directly. Whenever is high, the deposition is more successful, and this correlates with the X-ray diffraction analysis.

Co-Cr-Mo alloy considered as bioinert material and harm due to release of toxic ions such as Co and Cr ion inside the body, hence perform in osteolysis and allergenic reactions into body fluids.

Deposition of calcium phosphate, mainly by hydroxyapatite (HA) [$Ca_{10}(PO_4)_6(OH)_2$], on Co-Cr base alloy is considered as a promising method to enhance its biocompatibility , surface bioactivity [78], and direct bone formation with the adjacent hard tissue , It has also been demonstrated that HA reduces the release of potentially harmful metal ions, However, the use of sol-gel technique on Co based implants have not been reported although the use of other techniques, surface roughness it means creating massive voids between grains.

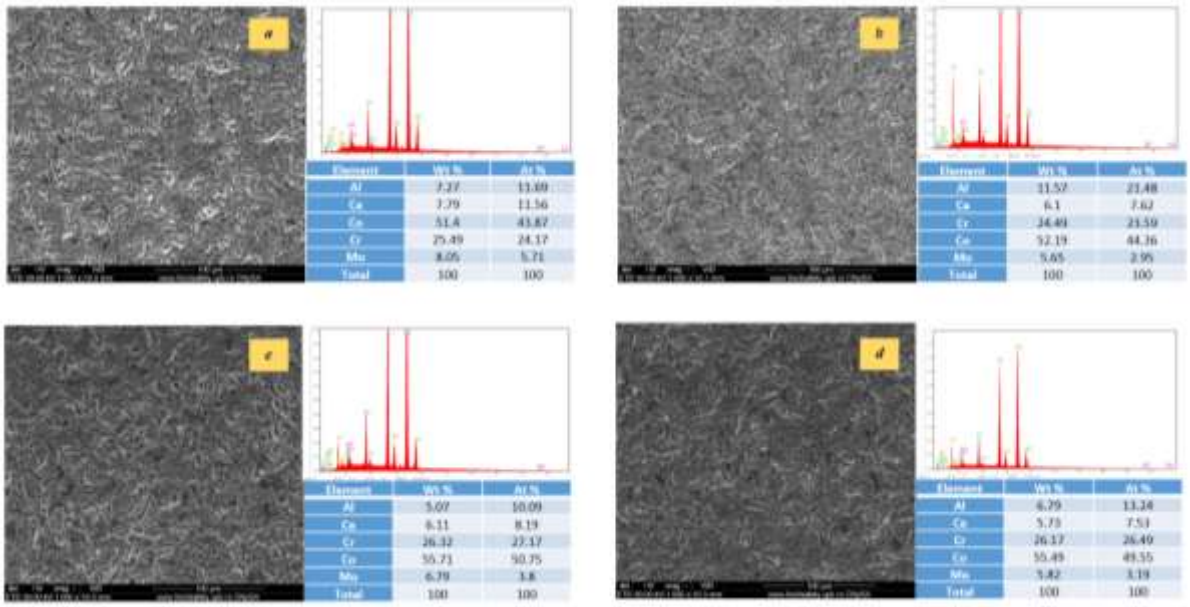

Fig. 4.18. The SEM micrographs and mapping registered for sample a) Hap_Ag_29 ^{Co}, b) HAp_Ag _45 ^{Co},C) HAp_Ag _110 ^{Co} , d)HAp_Ag _250 ^{Co}

B.4.3. Stabilization of thin films in SBF after 7, 14, and 21 days of immersion in SBF

The method of coating with HAp doped and undoped silver can be based on practical bio-mimicry by immersing implants in the simulated body fluid (SBF), which is an equal inorganic composition with the pH and temperature of the human blood plasma.

The surface morphology of the spinning coated specimens was observed by a field scanning electron microscope and X-ray spectra (XRD) analysis was performed.

B.4.3.1. X-ray Diffraction Analysis

B.4.3.1.1. HAp_29^{Co}-HAp_45 ^{Co} ,HAp_110 ^{Co} and HAp_ 250 ^{Co}

In ***figure 4.19***., the X-ray diffraction spectra of **HAp_29^{Co}**, **HAp_45^{Co}**, **HAp_110^{Co}**, HAp_250^{Co} after 7 days of immersion in SBF show the X-ray spectra of HAp_29^{Co} - HAp_250^{Co} for 7 days for analyzing the spectra of samples without silver, it be noticed that samples of HAp_29^{Co} and HAp_45^{Co} with roughness obtained by using particles of 29µm and 45µm respectively have a hydroxylapatite film with hexagonal crystal of calcium phosphate hydroxide $Ca_5(PO_4)_3(OH)$ according to ASTM datasheets 01-086-0740 and $Ca_4(PO_4)_2O$ as tetracalcium diphosphate monoxide, crystallizes in the monoclinic according to ASTM datasheets 01-084-9872 for HAp_45^{Co}, but with HAp_29^{Co} it crystallized with calcium phosphate hydroxide $Ca_5(PO_4)_3(OH)$, than the HAp_45^{Co} for intensity of diffraction lines for $Ca_4(PO_4)_2O$ decreases with increased roughness .

it can be seen that both samples of HAp_110^{Co} and HAp_250^{Co}, exhibit lower crystallinity compared to HAp_29^{Co} and HAp_45^{Co}, which is demonstrated by the intensity of smaller high diffraction lines, since the analyzed layer of HAp_110^{Co} and HAp_250^{Co} have shown the same formed of calcium phosphate $Ca_3(PO_4)_2$ with rhombohedral crystal structure according to ASTM datasheets 04-010-5151, indicating that stabilization of film has been good calcium phosphate TCP $Ca_3(PO_4)_2$, has long been considered as an excellent biomaterial to promote bone repairs and implant.

While theat samples without silver of HAp_45^{Co} after 14 days of spectra analyzing, with roughness obtained by using balls of 45µm formed calcium chromium oxide $CaCr_2O_4$ as Orthorhombic crystal according to ASTM datasheets 04-007-4990 that was also evidence of reaction of chromium from the alloys in SBF with released P, Cr ion as Orthorhombic and cubic crystal structures according to ASTM datasheets 03-065-2491 and 04-021-2342 respectively. while

HAp_110Co it crystallized with tricalcium phosphate.$Ca_3(PO_4)_2$, as rhombohedral crystal structure according to ASTM datasheets 04-010-5151 besides Co and Cr ion as tetragonal and cubic crystal structures according to ASTM datasheets 01-078-4003 and 04-021-2342 for intensity of diffraction lines for $Ca_3(PO_4)_2$ decreases with increased roughness .

it can be seen that sample of HAp_250^{Co}, exhibit lower crystallinity which is demonstrated by the intensity of smaller high diffraction lines, since the analyzed layer of HAp_250^{Co} have shown to formed calcium hydroxide $Ca(OH)_2$ with hexagonal crystal structure according to ASTM datasheets 01-073-6988 as portlandite responsible for the bioactivity and biocompatibility, thus means the precipitates of calcium hydroxide $Ca(OH)_2$ has been good, besides Co ion released as tetragonal crystal structure according to ASTM datasheets 01-078-4003.

Also for 21 days , as result of initially attracted of calcium ion to the negatively charged interface between the HAp coating and solution observed with HAp after 21 days, the calcium formed at the interface combines with phosphate ions, consequently forming apatite nuclei. With the increase of immersion time, a large amount of calcium ions and phosphate ions are attracted to the HAp coatings to form apatite precipitates $Ca_3(PO_4)_2$,Ca_5P_8,$C_{10}(PO_4)_6O$.

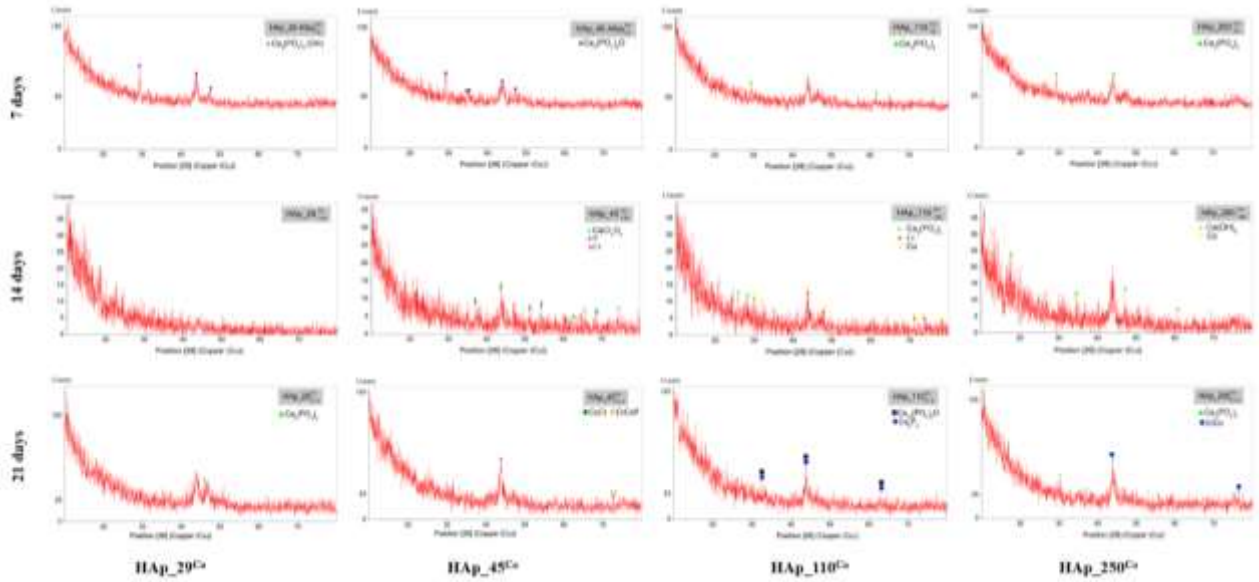

Fig. 4.19. Shows X-ray Diffraction Analysis of samples HAp_29^{Co}, HAp_45^{Co}, HAp_110^{co}, HAp_250^{Co} after 7, 14 and 21 days of immersion in SBF.

B.4.3.1.2 HAp_Ag_29^{Co}-Hap_Ag_45 ^{Co} ,HAp_Ag_110 ^{Co} and HAp_Ag_ 250 ^{Co}

In ***figure 4.20.*** the X-ray diffraction spectra of HAp_Ag_29^{Co}, HAp_Ag_45^{Co}, HAp_Ag_110^{Co}, HAp_Ag_250^{Co} after 7, 14 and 21 days of immersion in SBF.

It be noticed after 7 days , that sample of HAp doped silver HAp_Ag_29^{Co} which analyzed by X-ray spectra analysis had a tricalcium diphosphide compound of Ca_3P_2, as well as it has not been confirmed by X-ray crystallography, and silver Ag with cubic crystal structure according to ASTM datasheets 04-003-1472, while HAp_Ag_45^{Co} and HAp_Ag_110^{Co} contain tricalcium phosphate $Ca_3(PO_4)_2$ one of apatite family, with rhombohedral crystal structure according to ASTM datasheets 04-010-5151in addition to Ag as antibiotic agent with cubic crystal structure according to ASTM datasheets 04-003-1472 ,the only difference that HAp_Ag_110^{Co} released phosphorus with cubic crystal structure according to ASTM datasheets 04-016-6234 .

For samples HAp_Ag_250^{Co} where the roughness is obtained by particles size of 250µm, the diffraction spectrum shows that the stabilization was successful, with tricalcium diphosphide compound of Ca_3P_2, silver phosphide AgP_2 as monoclinic crystal structure according to ASTM datasheets01-076-1191 in addition to released Ag and P. At the same time, the intensity of the diffraction lines supports the high crystallinity of the samples.

While for 14 days, It be noticed that sample of HAp doped silver HAp_Ag_29^{Co} which analyzed by X-ray spectra analysis had a tricalcium phosphate $Ca_3(PO_4)_2$ with rhombohedral crystal structure according to ASTM datasheets 04-010-5151, and silver Oxide Ag_2O_3 as orthorhombic crystal structure according to ASTM datasheets 00-040-0909 which consequently leads to the antimicrobial activity besides Co ion released. While it has not been noted that HAp_Ag_45^{Co} had tricalcium phosphate $Ca_3(PO_4)_2$ with rhombohedral crystal structure according to ASTM datasheets 04-010-5151,and tetraphosphorus heptaoxide P_4O_7 with Monoclinic crystal structure according to ASTM datasheets 01-072-0984 in addition to the compound of calcium silver Ag_8Ca_3 with cubic crystal structure according to ASTM datasheets 00-028-0236 besides Co and Ag ions with cubic crystal structure according to ASTM datasheets 04-003-1472. for HAp_Ag_110^{Co} contain silver hydrogen phosphate Ag_2HPO_4, with hexagonal crystal structure according to ASTM datasheets 00-033-1183 which has an effect on the antimicrobial activity, and chromium cobalt $Cr_{0.7}Co_{0.3}$ with cubic crystal structure according to ASTM datasheets 04-002-1032, in addition to P ion orthorhombic crystal structure according to ASTM datasheets 03-065-249. wihle HAp_Ag_250^{Co} decomposed to calcium cobalt oxide $Ca_{0.47}CoO_2$ with anorthic crystal structure according to ASTM datasheets 04-017-4171 and silver calcium phosphide AgCaP with hexagonal crystal structure according to ASTM datasheets 00-033-1173 which provide surface bioactivity, besides to P and Ag ions released.so it noted that intensity of the diffraction lines supports the high crystallinity of the samples.

Also for 21 days, the effect of particles size which make the roughness of Co-Cr-Mo alloys on hydroxyapatite coated doped and undoped silver in SBF for different periods to create a different compounds of decomposed HAp, HAp_Ag_29^{Co}, HAp_Ag_45^{Co}, HAp_Ag_110^{Co}, HAp_Ag_250^{Co} which converted into more stable HAp. With increasing of immersion time to 21 days, HAp peaks have increased which confirms the growth of Hap

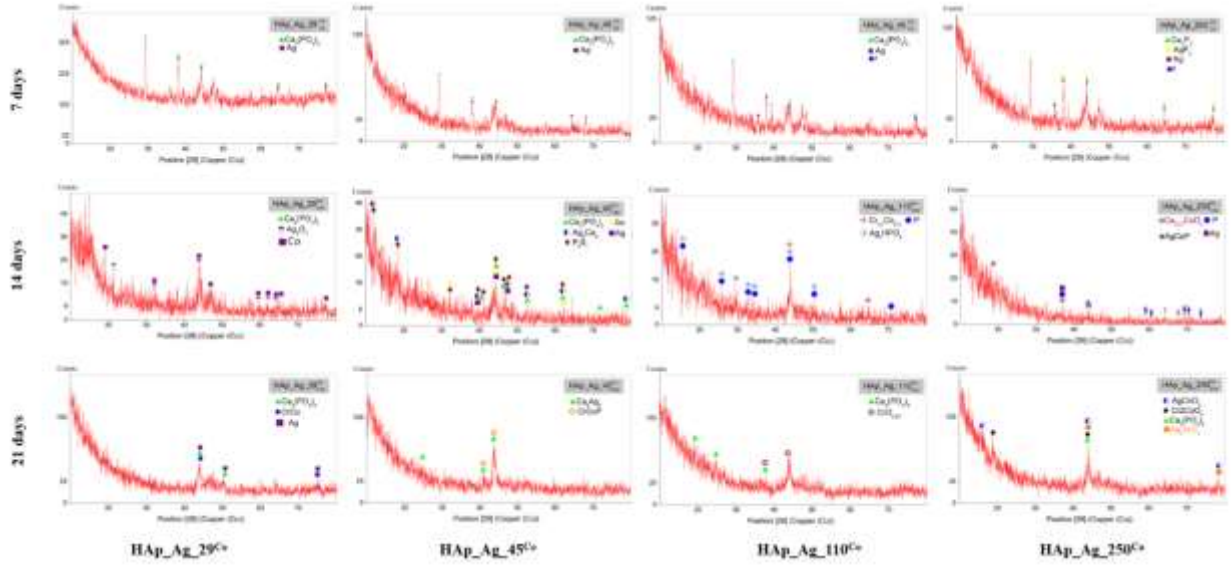

Fig. 4.20.shows the X-ray Diffraction Analysis of samples HAp_Ag_29^{Co}-Hap_Ag_45 ^{Co} ,HAp_Ag_110 ^{Co} and HAp_Ag_ 250 ^{Co} ^{Co} after **7, 14 and 21** days of immersion in SBF.

B.4.3.2. Scanning Electron Microscope (SEM)

B.4.3.2.1 HAp_29^{Co}-HAp_45 ^{Co} ,HAp_110 ^{Co} and HAp_ 250 ^{Co}

The below ***figure 4.21.*** which provide the scanning electron microscopy of HAp_29^{Co}, HAp_45^{Co}, HAp_110^{Co}, HAp_250^{Co} after 7,14. And 21 days of immersion in SBF.

According to SEM micrographs which performed after 7 days of immersion in SBF for HAp undoped silver, it can be seen in figure, that the calcium phosphate ceramics (biological apatite) film has developed quantitatively at the same time of presenting a homogeneous arrangement on

the surface of the **Co-Cr-Mo** alloys. This is an indication of high activity of hydroxyapatite in contact with physiological fluid in the human body. By comparison, it can be say that HAp_250^{Co} shows the best development of the formed film, so the roughness is directly involved in the stability of thin films.

While after 14 days of immersion in SBF, it can be see that the different films are formed with HAp different roughness, chromium oxide layer and phosphate ceramic film with ions released have a more significant development on the surface of the **Co-Cr-Mo** alloy substrate than the micrographs obtained 7 days after immersion, as well as HAp_110^{Co} and HAp_250^{Co} give a good morphology than others HAp.

The samples analyzed after 21 days of immersion in SBF, Focus of the success of deposition and growth of hydroxyapatite on **Co-Cr-Mo** substrate is being homogeneous with oxide layers.

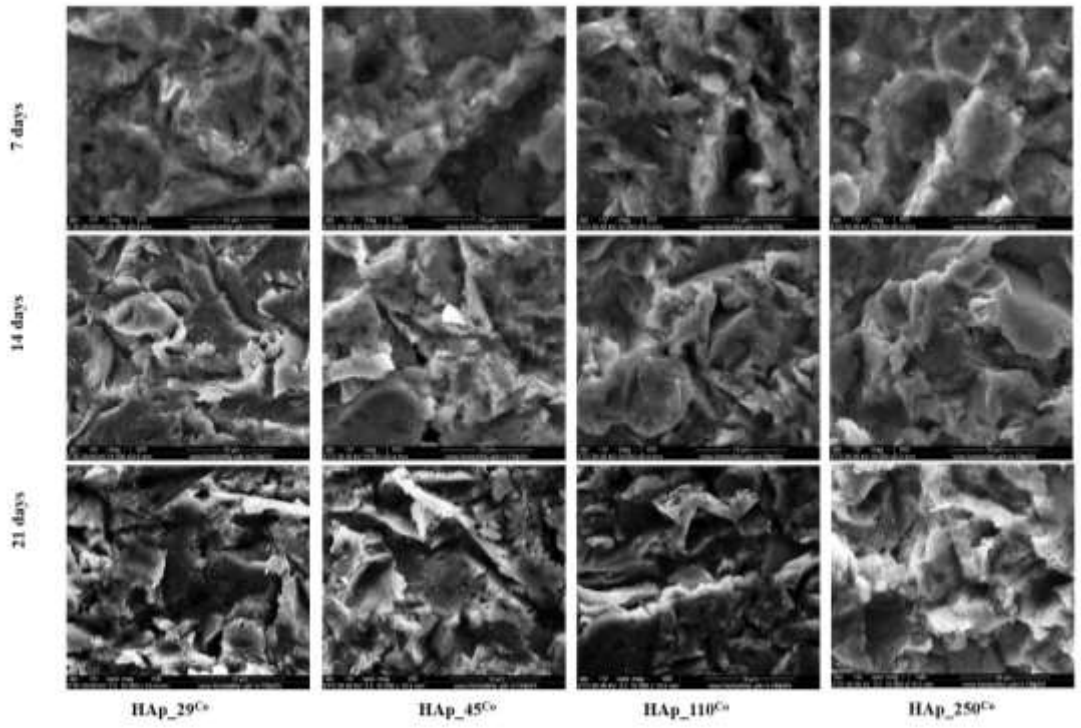

Fig. 4.21.shows the SEM analysis of samples HAp_29^{Co}, HAp_45^{Co}, HAp_110^{co}, HAp_250^{Co} after 7, 14 and 21 days of immersion in SBF.

B.4.3.2.2 HAp_Ag_29^{Co}-Hap_Ag_45 ^{Co} ,HAp_Ag_110 ^{Co} and HAp_Ag_ 250 ^{Co}

In the ***figure 4.22***. which provide the scanning electron microscopy of HAp_Ag_29^{Co}, HAp_Ag_45^{Co}, HAp_Ag_110^{Co}, HAp_Ag_250^{Co} after 7 days of immersion in SBF.

For samples doped with antibacterial agent silver, it is observed that after 7 days of immersion in SBF, the film of calcium phosphate ceramics grows significantly on all surfaces of the Co-Cr-Mo alloys. The morphology of SEM indicates a good particle size distribution of silver particles in surfaces homogenously, which is correlated with its release into the SBF solution "because growth of the thickness of film in SBF. The deposited film in SBF acts as nucleation growth, thus of calcium phosphate ceramic growth on the sample surfaces", as well as, the antibacterial action is more developed compared to the HAp undoped silver.in another side it can be noticed that HAp_Ag_250^{Co}is more stable than others because of AgP_2 is a source of antibacterial agent.

While after 14 days, it can be observed in significant amounts of thickness growth of film in SBF gradually with increased of surface roughness, the formation of additional film as a result of hydroxyapatite decomposition with oxides and hydroxides formation on the surface contribute to form silver particles on surface sa good particle size distribution homogenously.as well as with HAp_Ag_250^{Co} has another source for Ag agent by forming silver calcium phosphide.

After 21 days of immersion in the SBF, samples doped with silver no longer exhibit significant amounts of antibacterial agent. Only samples of HAp_110^{Co} and HAp_250^{Co} still contain silver

traces, correlated with the roughness of the substrates they have deposited, and thus the release activity is slower.

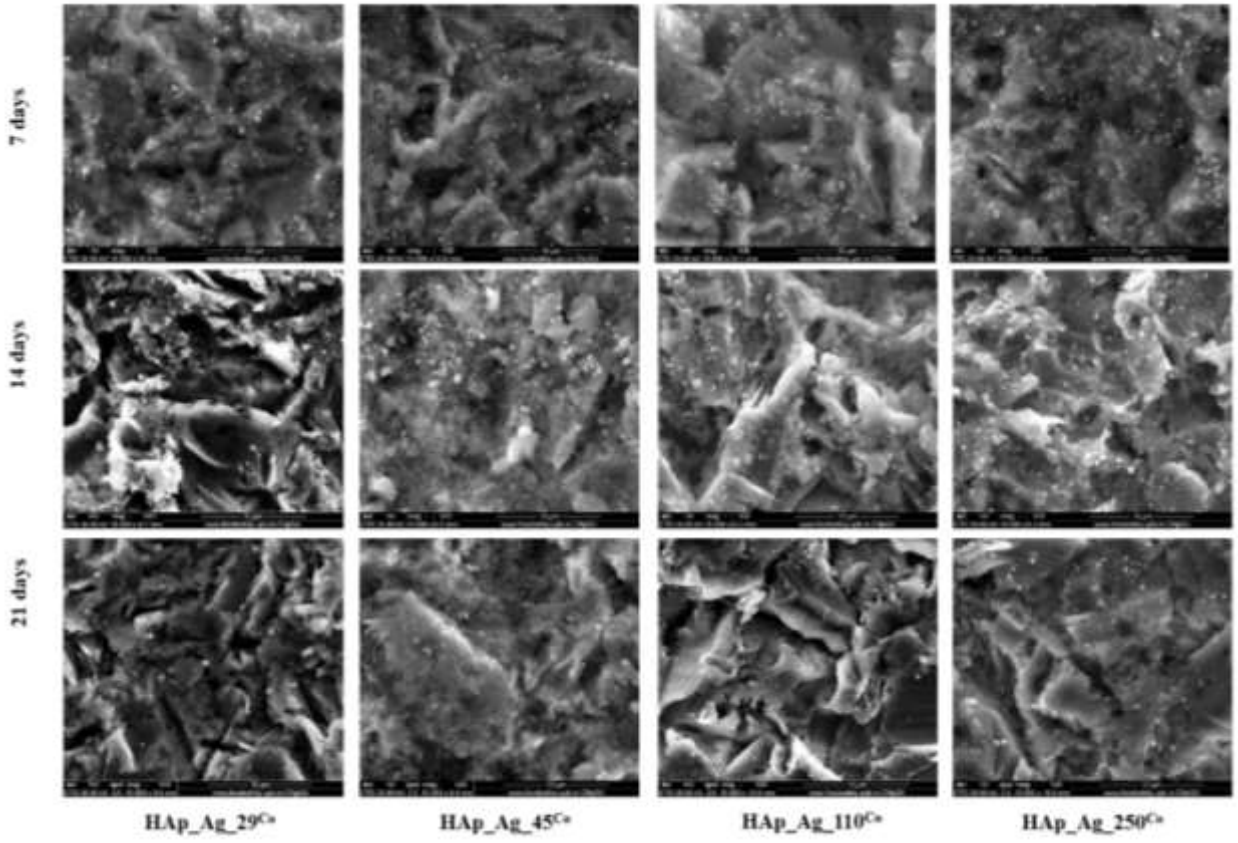

Fig. 4.22. shows the SEM analysis of samples HAp_Ag_29^{Co}, HAp_Ag_45^{Co}, HAp_Ag_110^{Co} ,HAp_Ag_250^{Co} after 7, 14 and 21 days of immersion in SBF.

B.4.4. Biological characterization

The effect of the materials obtained HAp^{Co} , and HAp_Ag^{Co} on the growth of microorganisms in liquid media (planktonic cultures) by using P.seudomonas aeruginosa strain by using a quantitative analysis of antimicrobial effect , while the effect of the surfaces obtained on the production of biofilms were analysed , in order to establish the antimicrobial activity of silver doped and undoped hydroxyaptite deposited on surfaces of Co-Cr-Mo alloy under differnent roughness sizes. The samples of test have been encoded with numbering CODs as shown in ***table 4.2.***

Table 4.2. shows the CODs of samples of biological analysis for HAp^{Co} , and HAp_Ag^{Co}

Code	11	12	13	14	15
Sample	HAp_Ag_29 ^{Co}	HAp_Ag_29 ^{Co}	HAp_Ag_29 ^{Co}	HAp_Ag_29 ^{Co}	HAp_29 ^{Co}
Code	16	17	18	19	20
Sample	HAp_45 ^{Co}	HAp_110 ^{Co}	HAp_250 ^{Co}	Ctrl	P.A CTRL

The samples of HAp^{Co} and HAp_Ag^{Co} obtained was measured after incubation for 24h at 37°C, the absorbance of planktonic cultures developed in the presence of the materials using a spectrophotometer at a set Absorbance of 600nm. From the obtained graph it can be observed that the sample HAp_Ag_29^{Co} exhibit the most significant growth inhibition effect on P. aeruginosa strain. However, all the materials which contain silver as antimicrobial agent possess a great activity against P. aeruginosa. Also, for the materials only with HAp^{Co} it can be argued that these materials still have antimicrobial effect, by inhibiting the growth of the strain cells as shown in ***figure 4.23.***

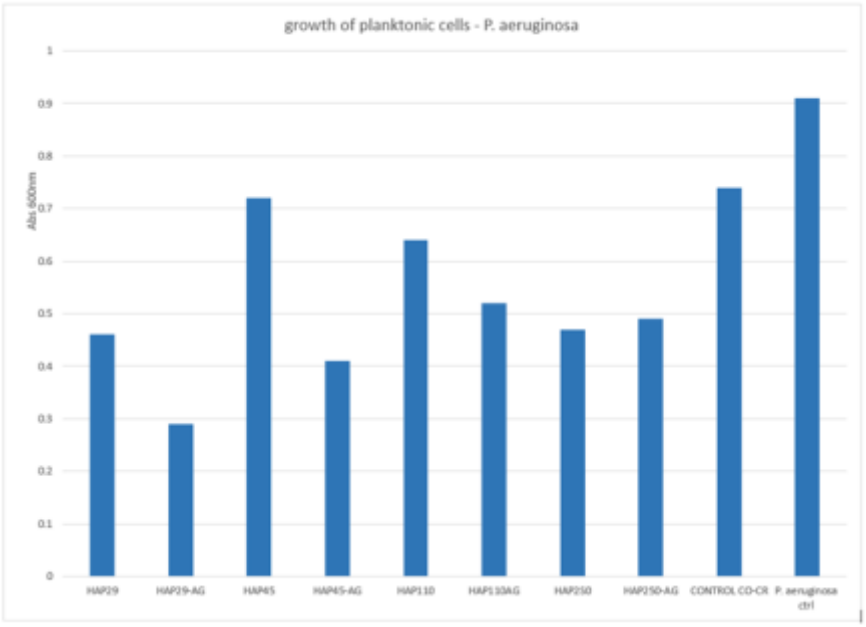

Fig. 4.23. Shows the Abs values at 600 nm suggesting the growth of planktonic microorganisms in the presence of **Co-Cr-Mo** based materials.

In the case of HAp^{Co} and HAp_Ag^{Co} samples as shown in ***figure 4.24***. the ability of the microbial cells to attach and develop biofilms after 24h of incubation was assessed, the obtained materials were tested by performing viable count analysis and calculate colony forming units/mL values. The results demonstrated that all the tested materials had an inhibitory effect against microbial attachment in *P. aeruginosa*. The most significant effect was observed for sample $HAp\_Ag\_45^{Co}$.

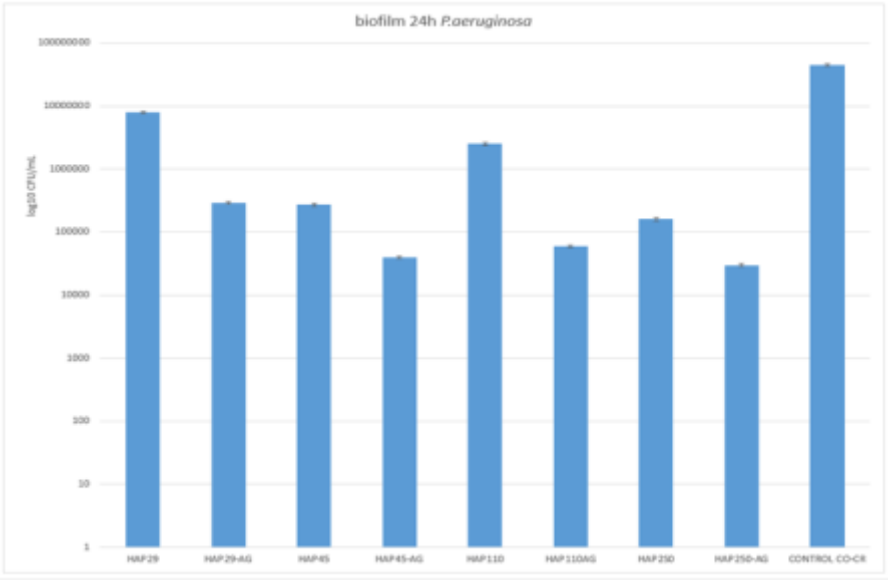

Fig. 4.2. Shows the graphical representation of UFC / mL values representing the development of biofilms on the tested surfaces of HAp^{Co}, and HAp_Ag^{Co}

CHAPTER 5. CONCLUSIONS and SUGGESTIONS

5.1. CONCLUSIONS

The results of working were presented and discussed in detail of previous chapter with respect to surface modifications of two important biomedical alloys which include Ti6Al4V and Co-Cr-Mo which used in many field of medical and the researchers give it a higher priority. But here the research finding can be summarized as follows:

1. The creating a different surface roughness on alloys adopted on particles sizes of alumina by blasting process technique which used before HA coating deposition by sol-gel technique to improve the bonding between substrate - ceramic (HA) and coating activity.
2. The difference in crystallinity which is noted for HAp_Ag_29^{Ti} where the roughness was obtained with 29μm particles higher than the sample HAp_Ag_45^{Ti}.
3. The samples of HAp_Ag_110^{Ti} and HAp_Ag_250^{Ti} have roughly equal proportions of calcium and silver, with deposition being successful.
4. The samples of HAp_Ag_110^{Ti} and HAp_Ag_250^{Ti} has the most significant antimicrobial effect on the P. aeruginosa strain,as well as, an inhibitory effect on bacterial action.
5. The component of Tricalcium diphosphate (TCP) $Ca_3(PO_4)_2$ was formed in holes due to the larger size of the particles for the case of HAp_29^{Ti} and HAp_45^{Ti}
6. The lower crystallinity of HAp_110^{Ti} and HAp_250^{Ti} compared to HAp_29^{Ti} and HAp_45^{Ti}, which is demonstrated by the intensity of smaller high diffraction lines.
7. The hexagonal structure of Apatite $Ca_5(PO_4)_3(OH)$ afford the stability of hydroxyapatite as an excellent biomaterial used for bone repair or implants.
8. The deposited layer formed on the surface of titanium support is uniform and distributed in all the recesses.
9. The roughness resulted by blasting process enhances the adhesive and bonding between Co-Cr-Mo surface and ceramic HAp successfully.
10. It is important to note that, increasing the surface roughness lead to form a crystal structures differ from one to the other which work to promote the effectivity of surface when coated with HAp.
11. The deposited layer formed on the surface of Co-Cr-Mo alloy is uniform and distributed in all the recesses.
12. The samples of HAp_110^{Co} and HAp_250^{Co} exhibit lower crystallinity compared to HAp_29^{Co} and HAp_45^{Co}, because of calcium phosphate of hydroxyapatite was formed in holes due to the larger size of the particles.
13. Ag+ ions have managed to destroy a strain of P. aeruginosa , and biofilm formation prevented which indicated to significant ability in antibacterial property
14. The antibacterial behavior of Ti6Al4V is more than Co-Cr-Mo, as results of silver cation released Ag+ which is completely substituted by Ca^{+2} in the phosphate ceramics.
15. The alloy of Ti6Al4V containing silver as preferred biomaterials which a better choice for the practical use to prevent implants associated infections.
16. In the case of HAp_Ag_45^{Co} , Increasing the quantity of silver lead to be more resistance against biofilm formation, when it compared with both alloys.
17. The morphology of Tricalcium phosphate crystal formed with β-TCP after 21 immersion days, has a more stable structure and higher biodegradation, faster degradation rate and higher solubility. Consequently, lead to increase the biocompatibility.

5.2. SUGGESTIONS FOR FUTURE WORK

1. In order to further evaluate the biological performance of the Ti6A4V and Co-Cr-Mo alloy, it is suggested to further study its osseointegration and antibacterial capability in vivo.
2. The use of appropriate methods to measure the properties of roughness and micro-hardness to illustrate the potential impact on the characteristics of Ti-6Al-4V and Co-Cr-Mo alloy with different roughness when it coated by silver doped and undoped hydroxyapatite.
3. Study of adhesive and cohesive properties of silver doped and undoped Hydroxyapatite deposited on different roughness of Ti6Al4V and Co-Cr-Mo surfaces.
4. Study the effect of copper as a substitute for silver as antibacterial agent, and make comparison between them.
5. Investigation of effect of silver nanoparticles ion implantation technology created byusing the directed beam onto the surface of Ti6Al4V and Co-Cr-Mo alloy before and after coating with hydroxyapatite.

5.3. RESULTS DISSEMINATION

5.3.1. Published papers

1. A. A. Harb, I. Ciuca, **Mohammed Alqasim** ALSABTI, "The Effect Of Tig Welding On Corrosion Behavior For U- Bend Specimens Of 316l Austenitic Stainless-Steel Joints In Saline," vol. 80, 2018.
2. ALEXANDRA CĂTĂLINA BÎRCĂ, IONELA ANDREEA NEACŞU1, ION CIUCĂ, **MOHAMMED ALQASIM** FAYEQ "Mg–Zn alloys, most suitable for biomedical applications" Rom J Morphol Embryol 2018, 59(1):49–54.
3. **Mohammed Alqasim** ALSABTI1, Ion CIUCA, Bogdan ŞTEFAN VASILE, "Effect of surface roughness Ti6Al4V modified by hydroxyapatite coating" Annals of the University Dunarea de Jos of Galati:
4. **Mohammed Alqasim** ALSABTI1, Ion CIUCA, Bogdan ŞTEFAN VASILE,"THE EFFECT OF DIFFERNET SURFACES ROUGHNESS OF Ti6Al4V ALLOY ON SILVER DOPED HYDROXYAPATITE COATING", scientific bulletin of Politehnica University of Bucharest (B).

5.3.2. International conferences participation

1. Alaa ABOU HARB, Ion CIUCA, **Mohammed ALQASIM** FAYEQ, Mihai VASILE., "corrosion behavior for u- bend samples of 304 austenitic stainless-steel joints which welded by TIG in saline solution", TEME 2019, 23th -25th of October, Galați, Romania, 4th Edition Of The International Conference "New Trends In Environmental And Materials Engineering".
2. **Mohammed ALQASIM** FAYEQ, Ion CIUCA, Bogdan ŞTEFAN VASILE, Alaa ABOU HARB, Roxana TRUSCA., "The effect of different surfaces roughness of ti6al4v alloy on silver doped hydroxyapatite coating", TEME 2019, 23th -25th of October, Galați, Romania, 4th Edition Of The International Conference "New Trends In Environmental And Materials Engineering.
3. **Mohammed ALQASIM** FAYEQ, Ion CIUCA, Bogdan ŞTEFAN VASILE, Alaa ABOU HARB, Roxana TRUSCA "EFFECT OF TITANIUM SURFACE ROUGHNESS MODIFIED BY HYDROXYAPATITE COATING "BraMat 2019,13th and 16th of March, 11th International Conference on Materials Science & Engineering.

Referances

[1] F. M. Chen and X. Liu, "Advancing biomaterials of human origin for tissue engineering," *Prog. Polym. Sci.*, vol. 53, pp. 86–168, 2016.

[2] L. Tian *et al.*, "Hybrid fracture fixation systems developed for orthopaedic applications: A general review," *Journal of Orthopaedic Translation*, vol. 16. pp. 1–13, Jan-2019.

[3] W. Sherman, "Vanadium steel bone plates and screws," *Surg Gynecol Obstet.*, vol. 14. pp. 629–34, 1912.

[4] N. Patel and P. Gohil, "A review on biomaterials: scope, applications & human anatomy significance," *Int. J. Emerg. Technol. Adv. Eng.*, vol. 2, no. 4, pp. 91–101, 2012.

[5] D. Bajenaru-Georgescu, D. Ionita, M. Prodana, and I. Demetrescu, "Electrochemical and antibacterial characterization of thermally treated titanium biomaterials," *UPB Scientific Bulletin, Series B: Chemistry and Materials Science*, vol. 77, no. 4. pp. 63–74, 2015.

[6] J. M. Morais, F. Papadimitrakopoulos, and D. J. Burgess, "Biomaterials/Tissue Interactions: Possible Solutions to Overcome Foreign Body Response," *AAPS J.*, vol. 12, no. 2, pp. 188–196, Jun. 2010.

[7] B. Priyadarshini, M. Rama, Chetan, and U. Vijayalakshmi, "Bioactive coating as a surface modification technique for biocompatible metallic implants: a review," *Journal of Asian Ceramic Societies*, vol. 7, no. 4. pp. 397–406, 02-Oct-2019.

[8] O. O. Ige, L. E. Umoru, and S. Aribo, "Natural Products: A Minefield of Biomaterials," *ISRN Mater. Sci.*, vol. 2012, pp. 1–20, 2012.

[9] L. S. Nair and C. T. Laurencin, "Biodegradable polymers as biomaterials," *Prog. Polym. Sci.*, vol. 32, no. 8–9, pp. 762–798, 2007.

[10] A. Sáenz, E. Rivera-muñoz, W. Brostow, and V. M. Castaño, "Ceramic Biomaterials : an Introductory Overview," *J. Mater. Educ.*, vol. 21, no. 5–6, pp. 297–306, 1999.

[11] U. Kamachimudali, T. M. Sridhar, and B. Raj, "Corrosion of bio implants," *Sadhana*, vol. 28, no. 3–4, pp. 601–637, 2003.

[12] J. Ni *et al.*, "Three-dimensional printing of metals for biomedical applications," *Mater. Today Bio*, vol. 3, p. 100024, Jun. 2019.

[13] H. Koizumi, Y. Takeuchi, H. Imai, T. Kawai, and T. Yoneyama, "Application of titanium and titanium alloys to fixed dental prostheses," *J. Prosthodont. Res.*, vol. 63, no. 3, pp. 266–270, Jul. 2019.

[14] B. Aygün, "High alloyed new stainless steel shielding material for gamma and fast neutron radiation," *Nucl. Eng. Technol.*, Aug. 2019.

[15] H. A. Zaman, S. Sharif, D. W. Kim, M. H. Idris, M. A. Suhaimi, and Z. Tumurkhuyag, "Machinability of Cobalt-based and Cobalt Chromium Molybdenum Alloys - A Review," *Procedia Manuf.*, vol. 11, pp. 563–570, 2017.

[16] S. L. Semiatin, V. Seetharaman, and I. Weiss, "Hot workability of titanium and titanium aluminide alloys—an overview," *Mater. Sci. Eng. A*, vol. 243, no. 1–2, pp. 1–24, 1998.

[17] S. L. De Assis, S. Wolynec, and I. Costa, "Corrosion characterization of titanium alloys by electrochemical techniques," *Electrochim. Acta*, vol. 51, no. 8–9, pp. 1815–1819, 2006.

[18] C. N. Elias, D. J. Fernandes, F. M. de Souza, E. dos S. Monteiro, and R. S. de Biasi, "Mechanical and clinical properties of titanium and titanium-based alloys (Ti G2, Ti G4 cold worked nanostructured and Ti G5) for biomedical applications," *J. Mater. Res. Technol.*, vol. 8, no. 1, pp. 1060–1069, Jan. 2019.

[19] R. Ion, D. Răducanu, M. L. Angelescu, A. Cîmpean, and R. M. Angelescu, "In vitro biocompatibility testing of three newly developed titanium alloys for oral implantology," *UPB Sci. Bull. Ser. B Chem. Mater. Sci.*, vol. 79, no. 2, pp. 207–216, 2017.

[20] I. Milošev, M. Metikoš-Huković, and H. H. Strehblow, "Passive film on orthopaedic TiAlV alloy formed in physiological solution investigated by X-ray photoelectron spectroscopy," *Biomaterials*, vol. 21, no. 20, pp. 2103–2113, 2000.

[21] A. Bandyopadhyay, F. Espana, V. K. Balla, S. Bose, Y. Ohgami, and N. M. Davies, "Influence of porosity on mechanical properties and in vivo response of Ti6Al4V implants," *Acta Biomater.*, vol. 6, no. 4, pp. 1640–1648, 2010.
[22] R. Lizárraga, F. Pan, L. Bergqvist, E. Holmström, Z. Gercsi, and L. Vitos, "First Principles Theory of the hcp-fcc Phase Transition in Cobalt," *Scientific Reports*, vol. 7, no. 1. 2017.
[23] P. Tolédano, G. Krexner, M. Prem, M. Prem, H. P. Weber, and V. P. Dmitriev, "Theory of the martensitic transformation in cobalt," *Physical Review B - Condensed Matter and Materials Physics*, vol. 64, no. 14. pp. 1441041–14410417, 2001.
[24] S. Jakobsen, A. Larsen, M. Stoltenberg, J. Bruun, and K. Soballe, "Effects of AS-cast and wrought cobalt-chrome-molybdenum and titanium-aluminium-vanadium alloys on cytokine gene expression and protein secretion in J774A.1 macrophages," *Eur. Cells Mater.*, vol. 14, pp. 45–55, Sep. 2007.
[25] L. H. M. Antunes *et al.*, "Effect of phase transformation on ductility of additively manufactured Co–28Cr–6Mo alloy: An in situ synchrotron X-ray diffraction study during mechanical testing," *Mater. Sci. Eng. A*, vol. 764, p. 138262, Sep. 2019.
[26] C.-L. Li, C. H. Park, S.-W. Choi, S.-W. Lee, J.-K. Hong, and J.-T. Yeom, "High strength and high ductility in the Co–20Cr–15W–10Ni alloy having a bimodal grain structure achieved by static recrystallization," *Mater. Sci. Eng. A*, vol. 732, pp. 70–77, Aug. 2018.
[27] J. Lu, V. J. Toplosky, R. E. Goddard, and K. Han, "Low temperature physical properties of Co-35Ni-20Cr-10Mo alloy MP35N®," *Cryogenics (Guildf).*, vol. 86, pp. 106–111, Sep. 2017.
[28] Q. Chen and G. A. Thouas, "Metallic implant biomaterials," *Mater. Sci. Eng. R Reports*, vol. 87, pp. 1–57, 2015.
[29] C. Knabe, C. R. Howlett, F. Klar, and H. Zreiqat, "The effect of different titanium and hydroxyapatite-coated dental implant surfaces on phenotypic expression of human bone-derived cells," *J. Biomed. Mater. Res. - Part A*, vol. 71, no. 1, pp. 98–107, 2004.
[30] D. Tlpeanu, A. Cojocaru, R. I. Zamfir Andronic, M. Bane, and S. Ciuca, "Comparative tests on corrosion resistance of some titanium-hydroxyapatite based nanocomposites," *UPB Scientific Bulletin, Series B: Chemistry and Materials Science*, vol. 78, no. 2, pp. 185–194, 2016.
[31] M. Ribeiro, F. J. Monteiro, and M. P. Ferraz, "Infection of orthopedic implants with emphasis on bacterial adhesion process and techniques used in studying bacterial-material interactions," *Biomatter*, vol. 2, no. 4, pp. 176–194, 2012.
[32] J. L. Hobman and L. C. Crossman, "Bacterial antimicrobial metal ion resistance," *Journal of Medical Microbiology*, vol. 64, no. 2014. pp. 471–497, 2015.
[33] X. Pang and I. Zhitomirsky, "Electrodeposition of hydroxyapatite-silver-chitosan nanocomposite coatings," *Surf. Coatings Technol.*, vol. 202, no. 16, pp. 3815–3821, 2008.
[34] T. T. Thanh, C. M. Cotrut, M. D. Vranceanu, E. Ungureanu, and M. Tarcolea, "Studies of microstructure and composition of modified hydroxyapatite coatings via sem investigations," *UPB Sci. Bull. Ser. B Chem. Mater. Sci.*, vol. 82, no. 1, pp. 145–154, 2020.
[35] C. I. Dragan, C. Pantilimon, E. E. Popa, G. Coman, and C. Gradinaru, "Green synthesis, characterization and antimicrobial of silver nanoparticles," *UPB Sci. Bull. Ser. B Chem. Mater. Sci.*, vol. 80, no. 4, pp. 267–275, 2018.
[36] S. Chen, S. Gururaj, W. Xia, and H. Engqvist, "Synthesis of Ag doped calcium phosphate particles and their antibacterial effect as additives in dental glass ionomer cements," *J. Mater. Sci. Mater. Med.*, vol. 27, no. 11, pp. 1–7, 2016.
[37] V. A. S. Rodica ROGOJAN, Ecaterina ANDRONESCU, "PREPARATION AND CHARACTERIZATION OF HYDROXYAPATITE NANOPOWDERS DOPED WITH SILVER IONS," *U.P.B. Sci. Bull., Ser. B*, vol. 78, no. 3, pp. 18–26, 2016.
[38] S. V. Dorozhkin, "Calcium orthophosphate cements and concretes," *Materials (Basel).*, vol. 2, no. 1, pp. 221–291, 2009.
[39] L. C. Palmer, C. J. Newcomb, S. R. Kaltz, E. D. Spoerke, and I. Samuel, "NIH Public Access," vol. 108, no. 11, pp. 4754–4783, 2009.

[40] S. S. S. SHEKHAR L. PANDHARIPANDE1, "Review on Synthesis of Hydroxyapatite and its Bio-composites," *Int. J. Sci. Eng. Technol.*, vol. 05, no. 17, pp. 3410–3416, 2016.
[41] L. C. Palmer, C. J. Newcomb, S. R. Kaltz, E. D. Spoerke, and S. I. Stupp, "Biomimetic systems for hydroxyapatite mineralization inspired by bone and enamel," *Chem. Rev.*, vol. 108, no. 11, pp. 4754–4783, 2008.
[42] E. Bash, "Advances in Materials Science and Implant Orthopedic Surgery," in *PhD Proposal*, vol. 1, 1995, p. 315.
[43] A. L. Boskey, "Bone composition: relationship to bone fragility and anti-osteoporotic drug effects," *BoneKEy Reports*, vol. 4. 2015.
[44] J. S. Al-Sanabani, A. A. Madfa, and F. A. Al-Sanabani, "Application of calcium phosphate materials in dentistry," *Int. J. Biomater.*, vol. 2013, no. May 2013, pp. 1–12, 2013.
[45] J. L. Ong, D. C. N. Chan, and K. Bessho, "HA Coatings on Dental Implants," in *Biomaterials Engineering and Devices: Human Applications*, Totowa, NJ: Humana Press, 2000, pp. 49–60.
[46] H. Zhou and J. Lee, "Nanoscale hydroxyapatite particles for bone tissue engineering," *Acta Biomater.*, vol. 7, no. 7, pp. 2769–2781, 2011.
[47] M. Okada and T. Matsumoto, "Synthesis and modification of apatite nanoparticles for use in dental and medical applications," *Jpn. Dent. Sci. Rev.*, vol. 51, no. 4, pp. 85–95, 2015.
[48] C. Rey, C. Combes, C. Drouet, H. Sfihi, and A. Barroug, "Physico-chemical properties of nanocrystalline apatites: Implications for biominerals and biomaterials," *Mater. Sci. Eng. C*, vol. 27, no. 2, pp. 198–205, 2007.
[49] BYSam Zhang, *Hydroxyapatite, Coatings for Biomedical Applications*. Advances in Materials Science and Engineering, 2013.
[50] E. Andronescu, A. Surugiu, M. L. Badea, C. S. Ciobanu, and A. Iosif, "Antimicrobial Activity of Europium Doped Hydroxyapatite Powders After Immersion in Sbf Solution," *U.P.B. Sci. Bull., Series B*, vol. 78. pp. 147–154, 2016.
[51] M. Prodana, D. Bojin, and D. Ioniţă, "Effect of hydroxyapatite on interface properties for alloy/biofluid," *UPB Sci. Bull. Ser. B Chem. Mater. Sci.*, vol. 71, no. 4, pp. 89–98, 2009.
[52] V. G. Vasilescu, B. Gălbinașu, and E. Vasilescu, "Aspects regarding the evolution and characteristics of some titanium alloys used in oral implantology," *UPB Sci. Bull. Ser. B Chem. Mater. Sci.*, vol. 81, no. 1, pp. 194–204, 2019.
[53] "INVESTIGATION ON QUALITY OF HYDROXYAPATITE ADHESION ON Amir," no. July, 2008.
[54] D. Liu, K. Savino, and M. Z. Yates, "Surface & Coatings Technology Coating of hydroxyapatite fi lms on metal substrates by seeded hydrothermal deposition," *Surf. Coat. Technol.*, vol. 205, no. 16, pp. 3975–3986, 2011.
[55] A. H. Choi and B. Ben-nissan, "Applications of Hydroxyapatite Nanocoatings and Nanocomposite Coatings in Dentistry," vol. 1, pp. 2–4, 2016.
[56] K. Kuroda and M. Okido, "Hydroxyapatite Coating of Titanium Implants Using Hydroprocessing and Evaluation of Their Osteoconductivity," *Bioinorg. Chem. Appl.*, vol. 2012, pp. 1–7, 2012.
[57] S. Nath, B. Basu, and A. Sinha, "A comparative study of conventional sintering with microwave sintering of hydroxyapatite synthesized by chemical route," *Trends Biomater. Artif. Organs*, vol. 19, no. 2, pp. 93–98, 2006.
[58] I. V. Antoniac, *Handbook of Bioceramics and Biocomposites*. Cham: Springer International Publishing, 2016.
[59] P. Leduc *et al.*, "Improved Mechanical Properties of Nanocrystalline Hydroxyapatite Coating for Dental and Orthopedic Implants," *Mater. Res.*, vol. 1112, pp. 2–7, 2009.
[60] A. L. Rias, C. Bouchard, F. Segonds, and S. Abed, "Design for additive manufacturing: A creative approach," in *Proceedings of International Design Conference, DESIGN*, 2016, vol. DS 84, pp. 411–420.
[61] M. E. Bahrololoom, M. Javidi, S. Javadpour, and J. Ma, "Characterisation of natural hydroxyapatite extracted from bovine cortical bone ash," *J. Ceram. Process. Res.*, vol. 10,

no. 2, pp. 129–138, 2009.
[62] A. R. Yasmin, D. Kalyani, and A. U.- Chennai, “Naturally Derived Porous Hydroxyapatite / Polymer Biocomposite of Cuttlebone and Eggshell for Dental and Orthopedic Applications,” *Int. J. Res. Appl. Sci. Eng. Technol.*, vol. 3, no. Vi, pp. 471–477, 2015.
[63] A. K. Nayak, “Hydroxyapatite synthesis methodologies: An overview,” *Int. J. ChemTech Res.*, vol. 2, no. 2, pp. 903–907, 2010.
[64] V. Pokropivny, I. Hussainova, and S. Vlassov, “Introduction to nanomaterials and nanotechnology,” *Introd. Nanomater. Nanotechnol.*, pp. 1–138, 2007.
[65] G. E. L. Processing, “Handbook of Sol-Gel Science and Technology: Processing, Characterization and Applications, Volumes I–III Set edited by Sumio Sakka (Professor Emeritus of Kyoto University). Kluwer Academic Publishers: Boston, Dordrecht, London. 2005. lx + 1980 pp. $1500,” *J. Am. Chem. Soc.*, vol. 127, no. 16, pp. 6135–6135, 2005.
[66] M. Niilo-R??m??, S. K??rkk??inen, D. Gasbarra, and T. Lappalainen, “Inclusion ratio based estimator for the mean length of the boolean line segment model with an application to nanocrystalline cellulose,” *Image Anal. Stereol.*, vol. 33, no. 2, pp. 147–155, 2014.
[67] M. D. Tyona, “A theorical Study on spin coating technique,” *Adv. Mater. Res.*, vol. 2, no. 4, pp. 195–208, 2013.
[68] Techische Fakultät Der Christian-Albrechts Universitat zu kiel, “Spin coating,” *Mater. Today*, vol. 5, no. 12, p. 62, Dec. 2002.
[69] N. Sahu, B. Parija, and S. Panigrahi, “Fundamental understanding and modeling of spin coating process: A review,” *Indian J. Phys.*, vol. 83, no. 4, pp. 493–502, 2009.
[70] N. Formica, D. S. Ghosh, A. Martinez-Otero, T. L. Chen, J. Martorell, and V. Pruneri, “Ultrathin oxidized Ti to increase stability and smoothness of Al doped ZnO transparent conductors for high efficiency indium-free polymer solar cells,” *Appl. Phys. Lett.*, vol. 103, no. 18, 2013.
[71] MicroChemicals, “Spin Coating of Photoresist,” *Web Broch.*, p. 4, 2013.
[72] S. Ssenyange, F. Anariba, D. F. Bocian, and R. L. McCreery, “Covalent bonding of alkene and alkyne reagents to graphitic carbon surfaces,” *Langmuir*, vol. 21, no. 24, pp. 11105–11112, 2005.
[73] J. F. Douglas and A. Karim, “Communications to the Editor the Roughness of Spin-Cast Polymer Films,” *Macromolecules*, pp. 4669–4672, 2001.
[74] “Ca9.303[PO4]6[OH]0.606·1.97H2O (Ca4.65[PO4]3[OH]0.3[H2O]) Crystal Structure - SpringerMaterials.” [Online]. Available: https://materials.springer.com/isp/crystallographic/docs/sd_1601371. [Accessed: 22-Feb-2020].
[75] P. Makvandi *et al.*, “Antimicrobial modified hydroxyapatite composite dental bite by stereolithography,” *Polym. Adv. Technol.*, vol. 29, no. 1, pp. 364–371, Jan. 2018.
[76] C. A. Beevers, “The crystal structure of dicalcium phosphate dihydrate, CaHPO 4 .2H 2 O,” *Acta Crystallogr.*, vol. 11, no. 4, pp. 273–277, Apr. 1958.
[77] Y. Su, I. Cockerill, Y. Zheng, L. Tang, Y.-X. Qin, and D. Zhu, “Biofunctionalization of metallic implants by calcium phosphate coatings,” *Bioact. Mater.*, vol. 4, pp. 196–206, Dec. 2019.
[78] M. Rezazadeh Shirdar, I. Sudin, M. M. Taheri, A. Keyvanfar, M. Z. M. Yusop, and M. R. A. Kadir, “A novel hydroxyapatite composite reinforced with titanium nanotubes coated on Co–Cr-based alloy,” *Vacuum*, vol. 122, pp. 82–89, Dec. 2015.